Title

Complex absorbing potentials within EOM-CC family of methods: Theory, implementation, and benchmarks

Journal

The Journal of Chemical Physics, 141(2)

ISSN

0021-9606

Authors

Zuev, Dmitry
Jagau, Thomas-C
Bravaya, Ksenia B
et al.

Publication Date

2014-07-14

DOI

10.1063/1.4885056

Peer reviewed

Complex absorbing potentials within EOM-CC family of methods: Theory, implementation, and benchmarks

Dmitry Zuev[a], Thomas-C. Jagau[a], Ksenia B. Bravaya[b], Evgeny Epifanovsky[a,c,d], Yihan Shao[d], Eric Sundstrom[c], Martin Head-Gordon[c], and Anna I. Krylov[a]

[a] Department of Chemistry, University of Southern California, Los Angeles, California 90089-0482

[b] Department of Chemistry, Boston University, Boston, Massachusetts 02215-2521

[c] Department of Chemistry, University of California, Berkeley, California 94720

[d] Q-Chem Inc., 6601 Owens Drive, Suite 105 Pleasanton, California 94588

A production-level implementation of equation-of-motion coupled-cluster singles and doubles (EOM-CCSD) for electron attachment and excitation energies augmented by a complex absorbing potential (CAP) is presented. The new method allows to treat metastable states within the EOM-CC formalism in a similar manner as bound states. The numeric performance of the method and the sensitivity of resonance positions and lifetimes towards the CAP parameters and the choice of one-electron basis set are investigated. We develop a protocol for studying molecular shape resonances based on the use of standard basis sets and a universal criterion for choosing the CAP parameters. Our results for a variety of π^* shape resonances of small to medium-sized molecules demonstrate that CAP-augmented EOM-CCSD is competitive relative to other theoretical approaches for the treatment of resonances and is often able to reproduce experimental results.

I. INTRODUCTION

Metastable electronic states are important in diverse areas of science and technology ranging from high-energy applications (plasmas, attosecond and X-ray spectroscopies) to electron-molecule collisions (interstellar chemistry, radiolysis, DNA damage by slow electrons). These states (called resonances) can be accessed when molecules are excited above their ionization threshold, via electron attachment to closed-shell species, or by core ionization.

A concise and pedagogical introduction to the topic as well as references to earlier reviews

can be found in Ref. [1]. From the quantum mechanical point of view, resonance states belong to the continuum part of the spectrum and, therefore, their wave functions are not L^2-integrable. Yet, their wave functions bear certain resemblance to the bound states within the interaction region (i.e., close to the nuclei). Using boundary conditions for the outgoing wave (Siegert or Gamow formalism, see Ref. [1]), one arrives at the following form of the resonance wave function:

$$\Psi(x,t) = e^{-iEt}\phi_R(x) = e^{-\Gamma t/2}e^{-iE_R t}\phi_R(x) \tag{1}$$

where the phase-isolated part $\phi_R(x)$ resembles a bound-state wave function in the interaction region and E_R and Γ (real and imaginary parts of the complex energy $E = E_R - i\Gamma/2$) determine resonance position and width. The latter is inversely proportional to the resonance lifetime. Thus, the resonances appear as solutions of the Schrödinger equation with complex energy [1–4]. One can arrive at the same concept of complex energy via a completely different formalism (Feshbach approach) based on a separation of the Hamiltonian into coupled bound and continuum parts; in this approach, the resonance is described as a bound state coupled with the continuum, and the complex energy emerges from solving a non-Hermitian eigenproblem with an effective Hamiltonian [5].

One can avoid the inconveniences of working with continuum functions or fiddling with boundary conditions by reformulating the problem using complex variables [2–4]. The most rigorous approach is the complex-scaling formalism [2, 6] in which all coordinates are scaled by a complex number $e^{-i\theta}$; however, practical applications of this method are limited by its extreme sensitivity to the one-electron basis set [7–11] as well as conceptual difficulties regarding the separation of nuclear and electronic motions of the scaled Hamiltonian [12–15].

These problems are avoided in an alternative approach in which the original (non-scaled) Hamiltonian is augmented by a complex potential $-i\eta\hat{W}$ devised to absorb the diverging tail of the resonance wave function [16–18]. In the complete basis set limit, these complex absorbing potential (CAP) methods yield exact resonance positions and widths in the limit of zero CAP strength η [19]. It can be shown that CAP methods are related to exterior complex scaling methods [20, 21].

The use of CAPs in practical calculations is complicated by possible reflections leading to false resonances, sensitivity of the results to the form of the CAP W, and a strong basis

set dependence [19, 22]. Furthermore, one has to determine an optimal value for η, which is usually achieved by calculating trajectories $E(\eta)$ and requiring $|\eta\, dE/d\eta| = \min$.

In terms more familiar to electronic structure practitioners, reflections can be described as perturbations of the resonance wave functions and, consequently, energies caused by a finite-strength CAP. Finite basis sets give rise to additional reflections. Several reflection-free CAPs have been proposed[19, 23]; such CAPs are either energy-dependent or non-local.

In our previous paper [24], we introduced a simple density-matrix based correction to the energy that removes the perturbation due to the CAP. The correction was derived based on energy decomposition analysis and response theory. Our starting point was the observation that the energy's dependence on η becomes roughly linear beyond some critical value of η. By analyzing the response equations, we also proposed an alternative criterion for finding an optimal value for η. Physically, our approach is grounded in the behavior of the resonance wave function and, ultimately, the one-particle density matrix. It was shown [24] that when the CAP is sufficiently strong, both real and imaginary parts of the density become near-stationary indicating that the resonance is stabilized. Then the perturbation to the resonance position by the CAP can be eliminated by subtracting the term $\eta\, Tr[\gamma W]$ from the energy. The optimal η is found by considering the de-perturbed resonance energies; moreover, we argued that η_{opt} is not the same for real and imaginary parts[24]. Preliminary benchmarks illustrated that this approach results in a computationally more robust scheme in which the dependence on the onset of the CAP is significantly reduced compared to the straightforward application of a CAP along with the original energy-based criterion for finding the optimal η, as was done in most CAP applications[25–27]. We note that Moiseyev *et al.* also observed a linear energy dependence on η beyond some critical value of η and proposed the use of Padé approximants to extrapolate the energy of the stabilized resonance to zero η limit[28, 29]. If the energy depends strictly linearly on η, their approach should give results identical to our first-order correction.

One of the difficulties of understanding the capabilities and limitations of different approaches is that a method that has shown excellent performance for a small model problem may fail when applied to a realistic system. In the context of electronic structure, the results of calculations of resonances will also be affected by the quality of standard approximations such as the incompleteness of one- and many-electron basis sets[30]. Thus, it is important to

test different methods for meta-stable states within robust and accurate *ab initio* approaches. For bound states, the coupled-cluster (CC) and equation-of-motion (EOM) hierarchies of methods [31–35] provide a reliable and predictive set of theoretical model chemistries [36]. These methods can be systematically improved to approach the exact solution, are size-extensive (or size-intensive for excitation energies), describe dynamical and non-dynamical correlation in one computational step, and do not involve system-dependent parameterization. The CC hierarchy of methods works best for wave functions dominated by a single Slater determinant, however, the EOM-CC approach extends this single-reference formalism to tackle various open-shell and multi-configurational cases[33, 37].

In EOM-CC the target-state wave function is described by an excitation operator $\hat{R}$ acting on the reference-state CC wave function:

$$|\Psi\rangle = \hat{R}e^{\hat{T}}\,|0\rangle \tag{2}$$

with $|0\rangle$ as the reference Slater determinant –usually satisfying the Hartree-Fock (HF) equations– and $\hat{T}$ as the coupled-cluster operator. Different choices of $\hat{R}$ provide access to different target states, e.g., in EOM-EE-CC $\hat{R}$ is electron and spin-conserving thus enabling the description of various excited states. Open-shell electron-attached states (such as temporary anions) can be described by EOM-EA-CC in which the reference state is again a well-behaved closed shell state and the operator $\hat{R}$ changes the number of electrons. Likewise, ionized states can be described by EOM-IP-CC with the operator $\hat{R}$ removing an electron. Thus, EOM-CC is a natural choice for extending the excited-state methodology to resonances via complex scaling and CAP approaches.

Recently, we presented an implementation of complex-scaled EOM-CCSD methods and illustrated their performance by considering several atomic systems (He, H^-, Be). Here we present an implementation of CAPs within the EOM-CCSD family of methods. Our main focus is on the EOM-EA-CC variant; however, our implementation also includes EOM-EE-CC. While limited implementations of CAPs within EOM-CC have been reported before (e.g., Refs. [25, 26]), this work presents the first formally complete and production-level implementation of the method.

The main focus of the paper is on investigating the numeric performance of the method and the sensitivity of the results towards the CAP parameters and the choice of basis set.

Our goal is to develop a black-box type approach that could be calibrated and then applied to the calculation of resonances without any prior knowledge of the system, as advocated by John Pople [36]. In particular, we want to avoid the system-dependent optimization of basis sets and the CAP's shape and onset. Thus, rather than aiming at results converged with respect to all computational parameters individually for each system, we wish to establish a uniform protocol that can be applied to any system and can be characterized by error bars estimated from prior calibration studies, as routinely performed in electronic structure calculations[30].

We note that the validation of the accuracy of computed resonance lifetimes in molecular systems is difficult[38]. A complete theoretical description should involve coupled electronic and nuclear dynamics; this is beyond the scope of the present paper, where we only compute the lifetime of the resonance state at a fixed molecular geometry. This is appropriate for resonances whose lifetimes are shorter than nuclear motions, or when nuclear motions do not strongly affect the computed Γ values (Condon-like approximation). Thus, our focus is on the comparison with other theoretical studies and the robustness of the results with respect to the one-electron basis set as well as variations of the CAP parameters.

In this context, we add that the sensitivity of the results towards the one-electron basis set is of a fundamentally different origin in CAP calculations as compared to complex scaling. In the latter case, the basis should be sufficiently flexible to describe the resonance wave function at different values of the scaling angle, whereas in the former case, one simply needs to supply a basis set of sufficient spatial extent to represent a given CAP and a stabilized resonance wave function. This implies that the diffuseness of the basis must be coordinated with the CAP onset, e.g., in a compact basis, the CAP onset should be smaller, otherwise, the calculation will be blind to the CAP. Thus, although the basis-set dependence is a nuisance, its simpler nature in CAP calculations suggests that a solution can be found.

Originally CAP methods were introduced to study shape resonances. Since the decay of Feshbach resonances is a two-electron process (and the CAP is a one-electron operator), one may expect difficulties in describing Feshbach resonances within the CAP formalism. Moiseyev *et al.* [39–41] showed that additional steps need to be taken for the construction of reflection-free CAPs in order to reliably calculate Feshbach-type resonances. The present paper focuses solely on understanding CAPs in the context of molecular shape resonances.

The article is structured as follows: Sections II and III present the formalism of CAP-

augmented EOM-CC calculations and our implementation. In Section IV, we put forward a protocol to determine resonance positions and lifetimes and investigate its robustness towards the choice of the one-electron basis set and the CAP's onset. In Section V, we subsequently apply our new scheme to a variety of molecular resonance states and compare the results to those obtained from experiment as well as using other theoretical approaches. Section VI provides concluding remarks.

II. THEORY

The basic idea of the CAP method [16–19] is the addition of an artificial complex potential to the original Hamiltonian:

$$H(\eta) = H - i\eta W \tag{3}$$

where W aims to absorbs an outgoing electron and η controls its strength. As in complex scaling [2–4, 11, 42], the addition of the CAP results in a non-Hermitian complex symmetric operator $H(\eta)$ [16] converting resonances into square integrable (L^2) wave functions. In our calculations we choose as CAP a quadratic potential with an unaffected region of cuboid (i.e., box) shape:

$$W = W_x + W_y + W_z \tag{4}$$

$$W_\alpha = 0 \quad \text{if} \quad |r_\alpha| < r_\alpha^0 \tag{5}$$

$$= (r_\alpha - r_\alpha^0)^2 \quad \text{if} \quad |r_\alpha| > r_\alpha^0$$

with r_α denoting the three Cartesian coordinates ($\alpha = x, y, z$). Thus, the CAP is controlled by 4 parameters: 3 parameters for the onset in each direction (r_x^0, r_y^0, r_z^0) and the strength η. In principle, the CAP strength is unbound ($\eta \in [0, \infty)$), but should be chosen such that the effect is large enough to absorb the wave function over a certain range, but not too large to prevent excessive perturbation of the wave function and the resonance energy [19].

In the complete one-electron basis set, the exact position of the resonance in the complex plane can be obtained as $\lim_{\eta\to 0} E(\eta)$ [16]. That is, an infinitesimally weak CAP, which is represented exactly (and, therefore, goes to infinity at large r), is sufficient to stabilize the resonance without perturbing it. Working with finite Gaussian basis sets requires one to perform series of calculations for different η in order to find an optimal value of the

strength parameter η_{opt} along the η-trajectory and the corresponding value of the resonance energy $E(\eta_{\text{opt}})$. A commonly used criterion for determining the optimal value of the strength parameter η is finding the minimum of the logarithmic velocity [16, 19]:

$$v(\eta) = |\eta \frac{\partial E(\eta)}{\partial \eta}| \tag{6}$$

Unfortunately, the position and width of the resonance computed using this criterion are very sensitive to the CAP onset [17, 24, 27] and thus does not provide a black-box approach. In our recent paper[24], the first-order deperturbative correction to the raw zeroth-order resonance energies E^R and E^I was introduced as:

$$U^R(\eta) = E^R(\eta) - \eta \text{Tr}[\gamma^I(\eta) W] \tag{7}$$

$$U^I(\eta) = E^I(\eta) + \eta \text{Tr}[\gamma^R(\eta) W] \tag{8}$$

with $\gamma(\eta)$ as the one-particle density matrix. The correction is based on perturbation theory; it removes the explicit dependence on the CAP from the computed resonance energies. As was illustrated in Ref. [24], the corrected energies, $U^R(\eta)$ and $U^I(\eta)$, exhibit nearly constant behavior for large η (that is, past the stabilization point, when the resonance wave function does not change much anymore); furthermore, the corrected trajectories computed using different CAP onsets become much more similar in the asymptotic region as opposed to the uncorrected trajectories, $E^R(\eta)$ and $E^I(\eta)$.

By looking separately at the real and imaginary parts of the deperturbed energy (U^R and U^I) as a function of η, we showed that the energy becomes near stationary at certain values of optimal strength (η^R_{opt} and η^I_{opt}) giving the position and lifetime of the resonance. Our results showed that this recipe leads to values for the resonance position and lifetime that are less sensitive to the CAP onset and thus more robust than the zeroth-order values E^R and E^I [24].

In our method the CAP is introduced at the HF level of theory, where we obtain a set of complex molecular orbitals (MOs) as the solution for a given strength η. Hence, a complex Koopmans' theorem holds for the virtual orbitals, i.e., they can be interpreted as zeroth-order approximation of the resonance state.

As the next step we solve the CCSD equations for the reference state [31, 32, 43–45] using $H(\eta)$:

$$(\Phi_\mu|e^{-T}H(\eta)e^{T}|\Phi_0) = (\Phi_\mu|\bar{H}(\eta)|\Phi_0) = 0 \tag{9}$$

with Φ_μ denoting the excited determinants. The resulting amplitudes t^η are also complex.

To compute electronically excited and electron-attached resonance states we use EOM-EE-CCSD and EOM-EA-CCSD [33, 46–50] methods that provide accurate and predictive descriptions for such target states. The wave function of the resonance state is found by solving a non-Hermitian eigenvalue problem for the right eigenvectors:

$$(\Phi_\mu|(\bar{H}(\eta) - E^\eta_{cc})R^\eta|\Phi_0) = R^\eta_\mu\Omega^\eta \tag{10}$$

which yields a set of complex amplitudes R^η, and complex excitation energies Ω^η. The latter are the raw, η-dependent resonance energies (which are equal to the difference between the total energy of the excited/attached EOM-CCSD state and the reference CCSD energy for a given η).

We note that for moderate CAP strengths and CAP onsets comparable with the spatial extent of the electron density of the reference state, the perturbation to the reference CCSD energy is small (10^{-5} a.u.) in contrast to complex-scaled calculations [11]. To compute the first-order correction to the raw resonance energies, the one-electron density matrix needs to be calculated. We employ an unrelaxed one-electron EOM-CCSD density matrix containing no amplitude- or orbital-response terms [51]:

$$\gamma_{pq}(\eta) = \frac{1}{2}\,(0|L^\eta e^{-T^\eta}\{p^+q + q^+p\}\,e^{T^\eta}R^\eta|0) \tag{11}$$

where L^η and R^η are the left and right EOM-CCSD eigenvectors, respectively.

Because of the non-Hermitian nature of $\bar{H}$ left eigenvectors have to be computed and biorthogonalized against the right eigenvectors in order to compute the density matrix:

$$(\Phi_0|L^\eta(\bar{H}(\eta) - E^\eta_{cc})|\Phi_\mu) = \Omega^\eta L^\eta_\mu\ , \tag{12}$$

$$(L_i|R_j) = \delta_{ij}\ , \tag{13}$$

where i and j denote different electronic states. Once the density matrix is computed, the

energy of the resonance state is corrected according to Eqs. (7) and (8).

The equations for CAP-CCSD and CAP-EOM-EE/EA-CCSD are identical to the original CCSD and EOM-EE/EA-CCSD equations except that all the input quantities such as the Fock matrix, the two-electron integrals, the MO matrix C, the T and R/L amplitudes are now complex and η-dependent. There is no need to add the CAP explicitly to the CCSD or EOM-CCSD equations since it is already included at the HF level.

In our paper on complex-scaled EOM-CC [11], we considered several variants of implementation, including the one in which the HF and CCSD equations for the reference state were solved for the unscaled Hamiltonian and the scaling was introduced only at the EOM-CC level. This required significant reformulation of the EOM-CC equations. By analogy, one may also consider an implementation of CAP-EOM-CC in which the CAP is introduced only at the EOM-CC level; this will be the subject of future work.

Due to the CAP, the Hamiltonian becomes non-Hermitian and complex symmetric, which necessitates using a different metric, the so-called complex symmetric scalar product (c-product) [16, 42, 52, 53], such that the variational principle is maintained:

$$(\psi_i|\psi_j) = \int \psi_i \psi_j dr \tag{14}$$

The difference to the regular scalar product is that the bra-vector is not complex conjugated. Mathematically, the c-product is a pseudoscalar product which does not induce a valid metric norm [42, 52]. However one can still define the c-norm $(f|f)$ which is, contrary to the regular norm, complex in general and might become zero for a non-zero function f ("self-orthogonality"):

$$(f|f) =< f_{re}|f_{re} > - < f_{im}|f_{im} > +2i < f_{re}|f_{im} >= |a|e^{i\phi} \in \mathbb{C} \tag{15}$$

where $< | >$ is a regular scalar product which is equivalent to the c-product for real functions. Thus, the normalization of all vectors (for example left and right EOM-CC eigenvectors) is done by multiplying by a complex number [42]:

$$\hat{f} = |a|^{-\frac{1}{2}} e^{-i\phi/2} f \tag{16}$$

resulting in $\hat{f}$ being a normalized vector. As mentioned above, use of the c-norm may lead

to "self-orthonormality" ($(f|f) = 0$ for $f \neq \vec{0}$), but this has not been observed in practice. Orthogonality is defined for the c-product in the same manner as for scalar product as $(f|g) = 0$ (c-orthogonality).

III. IMPLEMENTATION

The suite of CAP-EOM-CC methods has been implemented in the Q-Chem electronic structure package [54, 55] and has been released in version 4.2. For all complex CCSD and EOM-EE/EA-CCSD equations the libtensor library [56] for high-performance tensor operations has been used.

The calculations begin by solving the CAP-augmented restricted HF equations (CAP-RHF). CAP-RHF has been implemented as an extension to regular RHF using the object-oriented SCF library SCFman [57] in Q-Chem that employs the Armadillo linear algebra library [58] for matrix computations. We add that an adaptation of our implementation for CAP-UHF will be straightforward. The CAP is introduced as an additional term in the regular Fock matrix:

$$F^{\eta}_{\mu\nu} = F^{0}_{\mu\nu} - i\eta W_{\mu\nu} \tag{17}$$

The molecular orbitals must satisfy the following orthonormalization condition in the c-product metric:

$$(C^{\eta})^{T} S C^{\eta} = I \tag{18}$$

where S is the overlap matrix in the atomic orbital (AO) basis and $(C^{\eta})^{T}$ is transposed but not conjugated. Since the augmented Fock matrix F^{η} is non-Hermitian, the orbitals obtained using standard linear algebra routines for the diagonalization of general matrices are not normalized. In order to satisfy the orthogonality condition [Eq. (18)], the MOs are orthogonalized by using a modified Gram-Schmidt procedure with projections calculated using the c-product.

The Fock matrix $F^{\eta}_{\mu\nu}$ and the two-electron integrals $(\mu\nu|\lambda\sigma)$ are transformed into the MO basis by applying the complex orbital transformation matrix, $C^{\eta}_{\mu p}$; thus, these quantities become complex in the MO basis. The calculations proceed by solving the CCSD amplitude equations using a DIIS procedure [59] adapted for complex algebra with c-product. Once the complex t-amplitudes are converged, we find the excited-state energies and right eigenvectors

by using Davidson's procedure [60] generalized for non-Hermitian complex matrices. Note that the original $\bar{H}$ matrix is also non-Hermitian but real, thus, one only needs to modify the procedure to make it work with complex quantities and the c-product. We observe that for large values of η the convergence of Davidson's procedure is sometimes problematic, likely due to more pronounced non-Hermiticity. However, we were always able to converge a reasonable number of roots (2-10) by tweaking the parameters of Davidson's procedure such as subspace size, residual inclusion threshold, etc. Since the one-electron density matrix is needed for the calculation of the first-order correction to the energies, we also solve for the left eigenvectors using Davidson's procedure, as well as for left and right eigenvectors together to ensure their c-biorthogonality [Eq. (13)].

The CAP is evaluated in the AO basis through numerical quadrature using a Becke-type grid [61] of (99, 590) points (99 radial points and 590 angular points per radial point). Currently, we have implemented a shifted quadratic potential $(r - r_0)^2$ for a rectangular cuboid [Eqs. (4) and (5)], but our implementation allows for an easy extension of the shape of the unaffected region as well as the type of potential, e.g., higher order monomials $(r-r_0)^4$, $(r - r_0)^6$, etc. Our implementation also includes the optional addition of a real potential to the CAP, as was advocated in Ref. [41].

Relative to the conventional CCSD and EOM-CCSD methods, the addition of the CAP does not change the scaling of the computational cost [$O(N^6)$ for CCSD and EOM-EE-CCSD, $O(N^5)$ for EOM-EA-CCSD] or the memory requirements [$O(N^4)$]. However, because we need to work with complex numbers, the computational cost increases roughly by a factor of 4 and the storage requirements increase by a factor of 2. Furthermore, computation of the first-order energy correction requires the left eigenvectors, which increases the computation time relative to EOM-CCSD energy calculations. Another possible issue arises when the resonance state is lying high in energy, so that the Davidson procedure will need to find all lower roots and it might require a lot of iterations to converge. To solve this issue, we have implemented iterative solvers for interior eigenstates for conventional EOM-CCSD methods. Implementation of the interior eigenvalue solvers for CAP-EOM-CC methods is a subject of future work. Finally, the necessity to compute η-trajectories requires to run calculations for different values of η, but these calculations can be performed independently and can therefore be run in parallel.

IV. BENCHMARK CALCULATIONS

The necessity to find optimal values for the strength and the onset of the CAP as well as a pronounced basis set dependence of the results have prevented routine applications of CAP-based methods so far. Hence, investigating the numeric performance of CAP-EOM-CCSD, in particular with respect to the two aforementioned issues, is crucial for it to become a useful tool for studying resonances.

As for the one-electron basis set, it has been established that the straightforward application of standard basis sets yields poor results. Additional diffuse functions need to be incorporated for two reasons: (i) to obtain a sufficiently good basis-set representation of the CAP and (ii) to describe the outgoing electron correctly [16, 19, 62]. Owing to these requirements, CAP-based computations were often carried out using non-standard basis sets [26, 27, 62–67]. While such approaches are able to provide results that agree with experiment for some resonance states, a treatment based on standard basis sets not involving any optimization procedure would be superior as it is of black-box type, has predictive power, and is also computationally less demanding. Since the shape of the resonance wave function is similar to a bound-state wave function in the interaction region, it should be possible to lessen the basis-set dependence to the degree observed in regular EOM-CCSD calculations.

Concerning the choice of the CAP onset, one has to realize that the artificial nature of the CAP implies that it is impossible to deduce from basic physical laws a universally applicable procedure for finding optimal parameters for the CAP strength, onset, and shape. While this is unsatisfying from a formal point of view, a pragmatic approach is to mitigate the dependence of the physically meaningful results on the artificial parameters as much as possible. Along these lines, we introduced a first-order correction [24] that was shown to desensitize resonance positions and widths to the choice of onset parameters by removing the perturbation due to the CAP. However, as this dependence cannot be removed completely, one has to develop a protocol for the unique and system-independent choice of the CAP onset to make CAP-EOM-CCSD applicable in a routine manner.

A. Computational Details

In the following we examine the π^* shape resonances of CO^- and $C_2H_4^-$ using different basis sets and CAP onsets. Both states arise from adding an electron to the lowest unoccupied valence MO (LUMO) of the respective neutral molecule. Bond lengths and angles were chosen as R(CO) = 2.1316 a.u. for carbon monoxide and R(CC) = 2.5303 a.u., R(CH) = 2.0522 a.u., and $\angle$(CCH) = 121.2° for ethylene. All electrons were active in the correlation treatment. The CAP strength η was varied with a step size between 0.0001 a.u. and 0.001 a.u. Optimal values for η were determined according to the criterion from Eq. (6) as well as using the procedure outlined in Ref. [24]. The respective results are referred to as zeroth-order and first-order in all tables and in the discussion below.

The basis sets used in our calculations were derived from the aug-cc-pVXZ (X = D, T, Q, 5) series [68] through augmentation by additional even-tempered basis functions. In all cases, the exponents for the first additional basis functions were obtained as one half of the exponent of the most diffuse basis function with the same angular momentum in the parent aug-cc-pVXZ basis set. The exponents for the remaining additional basis functions were calculated as one half of the exponent of the preceding function.

We explored two different series of basis sets, namely one where we augmented the basis sets for all atoms except for hydrogen (denoted as (A) below) and one where we placed only one set of diffuse functions with averaged exponents in the center of the molecule (denoted as (C) below). Since the second approach is computationally less demanding, it is especially preferable when targeting larger systems. To ensure that this strategy does not give rise to artifacts, we computed EOM-EE-CCSD excitation energies for a number of bound excited states of CO and C_2H_4 using the aug-cc-pVTZ+3s3p3d(C) and aug-cc-pVTZ+3s3p3d(A) bases. The results are reported in Table I together with the corresponding values for $\langle R^2 \rangle$, which are helpful in distinguishing valence states from Rydberg states. As apparent from Table I excitation energies based on the two basis sets differ by not more than 0.04 eV for the very diffuse 4 $^1A_1$ state of CO and by just 0.001 eV for all other states considered. This shows that placing the additional diffuse functions in the center does not lead to inferior results for the bound excited states and thus suggests the application of this scheme to resonances. We note that a similar scheme has been employed before in the context of stabilization techniques [69, 70].

As for the choice of the CAP onset, we employed the square roots of the expectation values $\langle\alpha^2\rangle$ ($\alpha = x, y, z$) for the ground states calculated at the CCSD level of theory as a starting point and considered the impact of small variations. The values used are $r_x^0 = r_y^0 = 2.76$ a.u. and $r_z^0 = 4.97$ a.u. for CO and $r_x^0 = 7.10$ a.u., $r_y^0 = 4.65$ a.u., and $r_z^0 = 3.40$ a.u. for C_2H_4. The orientation of the molecules was chosen as follows: For CO the z-axis formed the molecular axis, whereas the C_2H_4 molecule was placed in the xy-plane with the CC bond oriented along the x-axis.

B. The Impact of the CAP Onset

Table II compiles resonance positions E_R and lifetimes Γ for the $^2\Pi$ resonance of CO^- and the $^2B_{2g}$ resonance of $C_2H_4^-$ obtained using the aug-cc-pVTZ+3s3p3d(C) basis and different values for the CAP onset. We started with the aforementioned values for r_α^0 based on the spatial extent of the ground-state wave function and then varied r_x^0, r_y^0, and r_z^0 independently. In addition to E_R and Γ, we report optimal CAP strengths as well as values for the norm of the CAP in the AO representation. As expected, the representation of the CAP becomes more complete for smaller values of r_α^0. In addition, the results for $||W||$, the Frobenius norm of the CAP matrix, show that the onset parameters are not all of the same importance: Consistent with the π^* character of the resonance states, r_z^0 makes the largest impact for $C_2H_4^-$ and $r_x^0 = r_y^0$ for CO^-. This trend is also reflected in all values for η_{opt}, E_R, and Γ: Varying the pivotal onset parameter by ± 0.5 a.u. shifts zeroth-order values for E_R by up to 0.028 eV and zeroth-order values for Γ by up to 0.048 eV, while the impact of the remaining onset parameters is roughly one order of magnitude smaller. We will thus focus on the onset parameter with the most pronounced influence in the remaining discussion.

Table II shows that both zeroth-order and first-order resonance positions and widths become smaller when increasing r_α^0, but we emphasize that these fluctuations are mitigated, especially for the width when considering first-order results: Here, E_R and Γ are both shifted by at most 0.025 eV upon variation of r_α^0. Also, it is apparent from Table II that smaller values for the CAP onset lead to smaller η_{opt} and that the first-order correction always entails larger values for η_{opt}. However, the relevance of the latter trends is debatable as the CAP strength η is not a physically meaningful quantity. One can argue along the same lines regarding the quantity $\eta \cdot dE/d\eta$ that needs to be minimized to find the optimal value for

η when using the conventional criterion from Eq. (6). As can be seen from Table II, trends in $\eta \cdot dE/d\eta$ are weakly pronounced and not uniform.

C. The Role of Diffuse Basis Functions

To analyze the convergence of resonance positions and widths with respect to the addition of diffuse basis functions, we studied the π^* resonances of CO^- and $C_2H_4^-$ using different augmentations. All results are summarized in Table III. The crucial role of the angular momentum of the additional basis functions becomes clear at the first glance: In the case of CO^-, a jump of almost 0.5 eV is observed for the zeroth-order resonance position when going from aug-cc-pVTZ+3s(C) to aug-cc-pVTZ+3s3p(C), while an additional augmentation by three sets of d-functions leads to a change of 0.06 eV. Three sets of f-functions on top of aug-cc-pVTZ+3s3p3d(C) shift E_R by just 0.007 eV. For the resonance width, d-functions play a more important role: Going from the 3s(C) to the 3s3p(C) augmentation changes Γ by 0.08 eV and the next step to 3s3p3d(C) changes Γ by 0.10 eV, but the value for 3s3p3d3f(C) differs from that for the preceding augmentation by just 0.004 eV.

For $C_2H_4^-$, the changes are in general of similar magnitude as for CO^-, but the big jump is observed when adding d-functions for both E_R and Γ. We add that similar trends are found for the first-order E_R and Γ of both resonance states. Also, we note that the use of basis sets with an augmentation including just s-functions (for CO^-) or just s and p-functions (for $C_2H_4^-$) entails much larger η_{opt} values and sizable differences between zeroth-order and first-order values. Finally, the importance of the angular momentum of the diffuse basis functions is also reflected in the $E(\eta)$ trajectories for $C_2H_4^-$ displayed in Figure 1. Their shape is altered considerably when d-functions are added, but is very insensitive towards the addition of p-functions or f-functions. These findings about the role of angular momentum can be easily related to the spatial symmetry of the resonance states and thus justify to choose an augmentation scheme based on symmetry considerations prior to the actual computations. In addition, we note that the values of $||W||$ show that adding basis functions with angular momentum higher than $\ell = 2$ does not significantly improve the basis-set representation of the CAP.

We also investigated the effect of adding more than three additional diffuse s, p, and d-functions. The corresponding results in Table III show that, while values for $||W||$ become

considerably larger indicating a more complete basis-set representation of W, the impact on resonance positions and widths does not exceed 0.035 eV except for one case: For $C_2H_4^-$, the zeroth-order E_R and Γ calculated using the augmentation schemes 3s3p3d(C) and 6s6p6d(C) differ by more than 0.1 eV. However, this discrepancy disappears when the first-order correction is applied. These results suggest that an accurate basis-set representation of the CAP near the interaction region is crucial for obtaining correct resonance positions and widths, whereas regions further away do not need to be covered by the basis set. Furthermore, since an increased dependence of E_R and Γ on the CAP onset is found in some cases, we conclude that it is neither necessary nor advisable to employ more than three additional sets of diffuse basis functions with the required angular momentum.

Table III also reports the results from a number of calculations with the aug-cc-pVTZ+3s3p(A) and aug-cc-pVTZ+3s3p3d(A) bases. Contrary to what we observed for bound states (cf. Table I), the differences between values for E_R and Γ obtained with the two augmentation schemes "C" and "A" are not negligible. Zeroth-order values differ by up to 0.23 eV and first-order values still by up to 0.15 eV. In one case, namely $C_2H_4^-$/aug-cc-pVTZ+3s3p, discrepancies of 0.4 eV are found, but this is probably related to the poor performance of the 3s3p augmentation scheme for $C_2H_4^-$ discussed earlier. However, we consider results obtained with the scheme "C" superior for several reasons: From the trajectories shown in Figure 2, one can see that the first-order quantities U^R and U^I enter the region of near-stationarity for smaller η, i.e., the resonance wave function shows faster convergence with respect to η, which is reflected in smaller η_{opt} values obtained in calculations using the augmentation scheme "C". Also, an increased dependence on the CAP onset is found in some cases when using scheme "A".

D. The Role of the Valence Basis Set

Besides the impact of additional diffuse functions, variations in the valence basis set also influence the results for E_R and Γ. This is illustrated by Table IV, which reports values for resonance positions and widths of the $^2\Pi$ resonance of CO^- and the $^2B_{2g}$ resonance of $C_2H_4^-$ computed using the aug-cc-pVXZ (X = D, T, Q, 5) bases, each one augmented according to the 3s3p3d(C) scheme. Concerning the resonance position, one can see that for both zeroth-order and first-order values the basis-set dependence is more pronounced than for

excitation energies corresponding to bound states of the neutral molecules. The position of the resonance state in CO^- still changes by 0.06 eV when going from aug-cc-pVQZ to aug-cc-pV5Z, whereas the largest shift observed for a bound state is less than 0.03 eV. We also note that the positions of the resonance states become smaller with increasing basis-set size, while the opposite is true for the excitation energies of the bound Rydberg states.

Concerning the resonance width, trends are less clear. For CO^-, both zeroth-order and first-order values show a non-monotonic behavior with respect to the basis-set size and no convergence is observed. The magnitude of the variations in Γ is however comparable to those in E_R. For $C_2H_4^-$ in contrast, the dependence of Γ on the basis-set size is much less pronounced and convergence seems to be reached. We also see that the dependence of both E_R and Γ on the CAP onset is somewhat mitigated when increasing the size of the valence basis set: For the aug-cc-pVDZ basis set, a decrease of r_x^0 and r_y^0 by 0.5 a.u. increases E_R and Γ of the $^2\Pi$ resonance of CO^- by 0.032 eV and 0.073 eV, respectively, whereas the same decrease leads to changes of just 0.025 eV and 0.026 eV when using the aug-cc-pVQZ basis. This should be contrasted with the contrary impact of additional diffuse functions discussed before. Table IV also shows that the values for η_{opt} decrease for larger basis sets, which is in line with that η_{opt} should be zero in the complete basis set limit [16].

To gain further insight into the dependence of E_R and Γ on the size of the valence basis set we performed an energy decomposition analysis for the $^2\Pi$ resonance of CO^- and the $^2B_{2g}$ resonance of $C_2H_4^-$ based on the following partition of the electronic Hamiltonian:

$$H = \underbrace{E_{\text{HF}} + \sum_{pq} F_{pq}\{p^\dagger q\}}_{\text{one-electron part}} + \underbrace{\frac{1}{4}\sum_{pqrs} \langle pq||rs\rangle \{p^\dagger q^\dagger sr\}}_{\text{two-electron part}} \tag{19}$$

where the CAP is considered as a part of F_{pq} and $\langle pq||rs\rangle$ stands for the two-electron integrals in MO basis. The expectation value of the one-electron part is then interpreted as one-electron energy, whereas the expectation value of the remainder represents the contribution from the EOM-EA-CCSD two-particle density matrix. The results are compiled in Table V. For the real part of the energy, this illustrates that the one-electron part converges significantly faster to the complete basis-set limit than the two-electron part, which suggests that the overall slow convergence of the total energy is mainly driven by an incomplete treatment of electron correlation. In contrast, for the imaginary part of the energy, the

one-electron and two-electron parts seem to diverge in opposite directions with increasing basis-set size. This holds true for both molecules, but whereas the trends roughly cancel out for $C_2H_4^-$, this is not the case for CO^- leading to a seemingly different behavior for the overall resonance width of the two systems.

One might be tempted to relate the basis set dependence of Γ to an insufficient description of the interaction of the resonance state with the continuum, but we point out that the addition of further diffuse functions has only little impact on E_R and Γ (cf. Section IV C), which suggests the opposite. In total, we feel that the behavior of Γ requires further investigation in order to develop a scheme for the extrapolation to the complete basis set limit, but such an extension is beyond the scope of the present article. We point out, however, that the variations in Γ observed for CO^- do not exceed 0.15 eV so that reliable computations are still possible based on our current approach.

V. APPLICATIONS

In this section, we will report resonance positions and widths for a number of shape resonances of small to medium-sized molecules and compare the results from our CAP-EOM-EA-CCSD scheme to those obtained using other theoretical approaches or through experiment. Systems included in this study are N_2^-, CO^-, $C_2H_2^-$, $C_2H_4^-$, CH_2O^-, CO_2^-, and $C_4H_6^-$. All these resonance states except for the last one are derived by electron attachment to the π^* lowest unoccupied molecular orbital of the corresponding neutral molecules. $C_4H_6^-$ (1,3-butadiene) is a special case as its π system extends over more than a single double bond, which results in two low-lying resonance states.

We add that only the real part of the resonance wave function has a well defined single-attachment character, while the imaginary part has a considerably different form. Most often, it exhibits multireference character and is dominated by several single attachments to very diffuse orbitals. Also, its dependence on the CAP strength is more pronounced than that of the real part. A detailed investigation of this phenomenon is beyond the scope of this article.

In all calculations, we employed the scheme developed in Section IV, i.e., we chose the CAP onset based on the spatial extent of the ground-state wave function and used the aug-cc-pVXZ+3s3p3d(C) bases. Computational details are compiled in Table VI.

A. $^2\Pi_g$ Resonance in N_2^-

The scattering of slow electrons by the N_2 molecule has been studied experimentally several times [71–78] so that the $^2\Pi_g$ resonance of N_2^- is rather well characterized. Consequently, this resonance has served as a testing ground for numerous theoretical approaches including stabilization techniques [69, 70, 79, 80], methods based on complex scaling [10, 81, 82], CAP-based schemes [16, 26, 27, 62–66] as well as further approaches [83–85]. Among other aspects, the impact of electron correlation on the resonance position and width [62] as well as their basis-set dependence [26, 62, 64] have been investigated in detail for this system. In addition, the resonance wave function has been studied over a wide range of different bond lengths and adiabatic excitation energies have been determined [10, 80, 86, 87]. The potential interplay of the $^2\Pi_g$ ground state of N_2^- with other resonance states has been also investigated [10, 88].

CAP-EOM-EA-CCSD results obtained for the resonance position and width are compiled in Table VII together with several values available from the literature. The optimal CAP strengths found in our calculations are 0.0015 (0.0037) a.u. for the zeroth-order result and 0.0119 (0.0025) a.u. and 0.0148 (0.0071) a.u. for the real and imaginary part of the first-order result obtained with the aug-cc-pVTZ+3s3p3d(C) (aug-cc-pVQZ+3s3p3d(C)) basis set. We refrained from including experimental results in Table VII except for the fixed-nuclei estimate by Berman *et al.* (E_R = 2.32 eV, Γ = 0.41 eV) [89], which has been often considered as the reference value in previous theoretical studies. We add that this value was not obtained directly from the experiment, but through a fit to the experimental data using Feshbach's projection operator formalism.

Table VII illustrates that a confusing plethora of values for the resonance position and width of the $^2\Pi_g$ state of N_2^- have been reported. One can see that our results obtained from CAP-EOM-EA-CCSD overestimate E_R relative to the value from Ref. [89], while Γ is underestimated. For our highest-level calculation (first-order CAP-EOM-EA-CCSD/aug-cc-pVQZ+3s3p3d(C)) the deviation is about 0.15 eV for E_R and 0.13 eV for Γ. For E_R such a deviation is generally considered acceptable for EOM-EA-CCSD when dealing with bound states. An assessment of the deviation in Γ is more difficult as a comparison to bound states cannot be made. The differences between our highest-level value and our remaining results show however that the basis-set size and the correction for the CAP potential both

make a sizable impact on E_R and Γ, but whereas these effects work in the same direction for the resonance position, the change in Γ is more involved. As for the first-order correction, the results obtained within the static-exchange approximation [16] exhibit trends similar to those observed in the present study.

Table VII also shows that most approaches gave rise to too high values for the resonance position, whereas the reference value for the resonance width from Ref. [89] was often surprisingly well reproduced. The impact of electron correlation is illustrated by the comparison of high-level correlated methods to lower levels of theory. The position of the resonance state is consistently calculated to be above 3 eV with HF, DFT, and CIS based methods, regardless of whether stabilization techniques, complex scaling, or CAPs are employed, while the use of correlated methods leads to a significantly better agreement with the reference value. The only notable exception is the complex-scaled MRCI result (1.38 eV) from Ref. [10], which is almost 1 eV below the reference value. Interestingly, CAP-augmented MRCI calculations [63] with a rather similar basis set yielded a quite different resonance position (2.97 eV).

Compared to its effect on the resonance position, the role of electron correlation for the width Γ is less clear. For example, the complex-scaled HF and CAP-HF calculations from Refs. [81] and [27] agree with the reference value within 0.03 eV and 0.015 eV, respectively, while some correlated calculations led to deviations of more than 0.2 eV [63]. In fact, it was stated explicitly [62] that several values reported in the literature might have benefitted from error cancellation. We note that most authors reported values for Γ that were higher than the reference value with some low-level approaches overestimating the width by a factor of more than two, whereas our calculations underestimated Γ.

Regarding the basis-set dependence, a comparison between different schemes is hampered by the fact that a variety of different basis sets has been used in previous studies. Bearing in mind our findings from Sec. IV D, it seems however justified to conclude for CAP-based methods that basis-set effects may account at least partly for the differences between values for Γ reported by different authors. In addition, the results from Ref. [80] suggest that, as compared to our CAP-augmented EOM-EA-CCSD scheme, the stabilization method combined with EOM-EA-CCSD leads to a somewhat faster convergence with respect to basis-set size. However, also the highest-level (aug-cc-pV5Z+3p) results obtained with the latter method ($E_R = 2.49$ eV, $\Gamma = 0.496$ eV) still show a sizable deviation from the reference

values.

B. $^2\Pi$ Resonance in CO^-

While we have employed the $^2\Pi$ resonance of CO^- as a test system in Section IV, we will consider it in this section with a different focus, i.e., we will compare our results to those obtained using other methods. In contrast to N_2^-, which has been studied frequently, comparatively few results have been reported for the isoelectronic CO^- [24, 26, 70, 82, 90–93]. Table VIII compiles the values available from the literature together with some representative values from Section IV.

Regarding the resonance position, Table VIII shows that most theoretical values are higher than the experimental value (1.50 eV) [78, 94] as in the case of N_2^-. Also, similarly to N_2^-, the resonance position is clearly overestimated in the static exchange approximation, in which electron correlation is neglected. Furthermore, CAP-EOM-EA-CCSD results obtained using different bases vary by up to 0.75 eV, which demonstrates the sizable impact of the basis set. We note, however, that our results obtained using the aug-cc-pVXZ+3s3p3d(C) bases approach the experimental value with growing basis-set size and that the first-order correction improves the resonance position with respect to experiment. Our highest-level result (1.762 eV, first order, aug-cc-pV5Z+3s3p3d(C) basis set) deviates from the experimental value by less than 0.3 eV.

The available values for the resonance width of CO^- differ by more than an order of magnitude as again illustrated by Table VIII. The largest value reported (1.65 eV) was obtained in the static exchange approximation, while the narrowest width (0.08 eV) was computed from the Σ^2 decouplings of the electron propagator, a pattern that is again similar to N_2^-. The CAP-EOM-EA-CCSD results for the resonance width from the present work and Refs. [26] and [24] vary by up to 0.68 eV, which illustrates once more the great influence of the basis set. As for the resonance position, the first-order correction improves the resonance width considerably with our highest-level result (0.604 eV, first-order, aug-cc-pV5Z+3s3p3d(C)) differing by 0.204 eV from the experimental value. However, we finally note that the experimental values for the resonance position and width of CO^- from Ref. [94] are not strictly comparable to the fixed-nuclei extrapolation for N_2^- from Ref. [89], which further complicates a rigorous assessment of the accuracy of theoretical approaches.

C. $^2\Pi_g$ Resonance in $C_2H_2^-$

$C_2H_2^-$ is a relatively well studied system and a number of theoretical [26, 80, 82, 95–97] as well as experimental [98–103] values for the resonance position and width are available from the literature. Those values as well as the results we obtained using our new CAP-EOM-EA-CCSD approach are compiled in Table IX. The optimal CAP strengths corresponding to our results are 0.0036 a.u. for the zeroth-order value and 0.0071 a.u. and 0.0058 a.u. for the real and imaginary part of the first-order value.

Table IX shows that our results for the resonance position are in qualitative agreement with those obtained from most experiments as well as from other theoretical approaches. Only when using the trapped electron method [98, 99, 103] considerably lower ($\sim$0.7 eV) resonance positions were found. Our zeroth-order CAP-EOM-EA-CCSD result (2.655 eV) agrees within 0.05 eV with the experimental values from Refs. [99], [100], and [102]. We note that the first-order correction lowers the CAP-EOM-EA-CCSD result for E_R by about 0.2 eV bringing it closer to the experimental value from Ref. [101], but basis-set effects may have an impact of similar magnitude.

Theoretical values for the resonance width vary between 0.19 eV and 1.11 eV and only two rough estimates of 0.8 eV [99] and >1.0 eV [100] are available from experiment. Our calculations qualitatively confirm these two estimates with the zeroth-order result (0.979 eV) being closer to one value and the first-order result (0.831 eV) being closer to the other value. As mentioned for the resonance position, basis-set effects may have a sizable impact so that an ultimate decision between the two experimental values cannot be made.

D. $^2B_{2g}$ Resonance in $C_2H_4^-$

Similar to CO^-, the $^2B_{2g}$ resonance in $C_2H_4^-$ has been chosen as a benchmark system in Section IV and here we will compare it with previously reported values. The $^2B_{2g}$ resonance in $C_2H_4^-$ has been studied quite extensively by both experimental [104–106] and theoretical methods [66, 67, 80, 107–110]. Experimental measurements by electron scattering and electron impact techniques [104–106] located the position of the $^2B_{2g}$ resonance around 1.8 eV with a width of $\Gamma = 0.7$ eV. Theoretically this resonance has been studied by a wide variety of methods including complex scaling [107, 109], CAP-based approaches [66, 67],

stabilization [80] as well as other techniques [108, 110]. The reported theoretical values vary from 1.77 to 2.62 eV for the position of the resonance and from 0.11 to 1.32 eV for the width, i.e., by more than an order of the magnitude in the latter case. All values along with the results from our method are summarized in Table X.

Similar to the trends observed for the previously discussed systems, the largest values for both position and lifetime are found by DFT in combination with the stabilization technique [80], whereas the shortest lifetimes are obtained when using electron propagator methods [110]. The resonance position obtained by CAP-EOM-EA-CCSD lies reasonably close (within 0.3 eV) to the experimental value (1.8 eV) for all basis sets used. Similar to results from EOM-CCSD calculations using stabilization techniques [80], the value of the resonance position is overestimated by CAP-EOM-EA-CCSD, but we observe a positive trend when enlarging the valence part of the basis set from triple zeta to quadruple zeta. Our best estimate for the position of the resonance (first-order CAP-EOM-EA-CCSD/aug-cc-pVQZ+3s3p3d(C)) is 1.903 eV, which differs from the experimental value by only 0.1 eV and is thus not worse than what is usually found in EOM-EA-CCSD calculations for bound states.

The resonance width calculated with CAP-EOM-EA-CCSD is underestimated in comparison to experiment by roughly a factor of two. However, similar to the position, enlargement of the valence basis set brings the theoretical value of the width closer to the experimental one. But in contrast to the position, the first-order correction worsens the value for the width as compared to experiment so that the best estimate from our calculations (0.373 eV, first-order CAP-EOM-EA-CCSD/aug-cc-pVQZ+3s3p3d(C)) still deviates by more than 0.3 eV. We add that we observed a similar underestimation of the resonance width in Section V A for N_2^-.

E. $^2B_1$ Resonance in CH_2O^-

Formaldehyde is of particular interest for our study since it is the smallest molecule containing the highly-polar carbonyl group, which means that an accurate description of polarization and correlation effects is especially important. Zeroth-order and first-order estimates of the position and the lifetime of the $^2B_1$ resonance state of CH_2O^- along with previous experimental and theoretical data are compiled in Table XI. The optimal CAP

strength for the zeroth-order CAP-EOM-EA-CCSD values is 0.01 a.u. and for the corresponding first-order values 0.024 a.u. and 0.021 a.u. for the real and imaginary part, respectively.

Experiments by electron transmission spectroscopy [111, 112] and vibrational excitation [113] report values of 0.86-0.87 eV for the resonance position. For the resonance width, no experimental value is available from the literature, but only an estimate based on electron collision experiments near 1 eV [113], which shows the lifetime to be of the same order of magnitude as the period of the ν_2 vibrational mode (0.216 eV for neutral formaldehyde [114]). This vibrational excitation (ν_2) corresponds to the CO stretch mode, which is mainly excited after autodetachment of the electron from the $^2B_1$ resonance state [113]. We deduce that the width of the resonance should be of the order of 0.1 eV as it is the case for the π^* resonances of the molecules discussed before.

Previously reported theoretical values vary from 0.682 eV to 3.0 eV for the position and from 0.1 to 0.794 eV for the width of the resonance [25, 115–120]. Similar to the molecules considered above, the static exchange approximation overestimates the position of the resonance by roughly a factor of three [115, 116]. This can be explained by the high polarity of the carbonyl group and the reorganization effects when the molecule undergoes electron attachment, which results in strong correlation between the incident electron and the electrons of the neutral formaldehyde and shows the need for an accurate treatment of electron correlation.

We also note that the smallest width (0.1-0.12 eV) is reported for electron propagator methods [117], a pattern similar to N_2^-, CO^- and $C_2H_4^-$. Our method yields resonance positions of 1.352 eV and 1.314 eV in zeroth order and first order, respectively, which is significantly higher than the experimental value, but close to the values obtained with the R-matrix method [118, 119]. The widths obtained with CAP-EOM-EA-CCSD are 0.376 and 0.277 eV in zeroth order and first order, which agrees best with the results from SAC-CI calculations [25]. However, the lack of experimental data prevents a more rigorous assessment of the values for the width obtained with our method.

F. $^2\Pi_u$ Resonance in CO_2^-

The scattering of slow electrons by the CO_2 molecule is well characterized experimentally [121–127]. Besides higher-lying resonance states, the existence of a $^2\Pi_u$ metastable state in the range of 3.8-4 eV was established. Theoretically, this system has been studied most often with a special emphasis on the changes when going from the linear to a bent structure, where the $^2\Pi_u$ state splits into a $^2A_1$ and a $^2B_2$ component [128–131]. The role of a virtual state near 2 eV [132] and the interplay with other resonance states [131] have also been investigated. Somewhat surprisingly, the position and width of the $^2\Pi_u$ resonance of the linear molecule have not yet been studied using high-level quantum-chemical methods but only within the static exchange approximation [133–136].

Table XII reports the results from the CAP-EOM-EA-CCSD calculations for the $^2\Pi_u$ resonance of linear CO_2^- along with theoretical and experimental values available from the literature. Optimal CAP strengths corresponding to our values are 0.0074 a.u. in zeroth order and 0.0295 a.u. (real part) and 0.0810 a.u. (imaginary part) in first order. One can see that CAP-EOM-EA-CCSD qualitatively reproduces the experimental values for the resonance position and also agrees within 0.2 eV with results from static exchange calculations. This is especially noteworthy as we observed in the preceding sections that the static-exchange approximation tends to overestimate the resonance position significantly. We also note that the impact of the first-order correction on the resonance position is relatively small (0.02 eV) as compared to the systems discussed above. With respect to the resonance width, Table XII shows that CAP-EOMEA-CCSD yields considerably smaller values than calculations in the static-exchange approximation, which can be related to the superior description of electron correlation in the former case. Also, the impact of the first-order correction on the width is sizable (0.08 eV). We finally point out that our first-order result for the resonance width (0.198 eV) agrees very well with the experimental value (0.20 eV) available from the literature [122].

G. ^2A_u and ^2B_g Resonances in $C_4H_6^-$

1,3-Butadiene is different from all species discussed before in that its π system extends over more than a single double bond. Two low-lying π^* resonances of ^2A_u and ^2B_g symmetry

result from this electronic structure, both of which have been characterized experimentally [104, 137]. However, while experimental values for the resonance position (0.62 eV and 2.82 eV) are available, no values for the width of either state have been reported in the literature. It was only concluded that the lower lying ^2A_u state should be longer lived as its spectrum exhibits vibrational structure. As for previous theoretical treatments of these resonances, only one study on the ^2A_u state employing conventional DFT/B3LYP, which found a surprisingly good agreement with experiment for the resonance position (0.76 eV), is available from the literature [138], but the resonance widths have apparently never been studied theoretically.

In Table XIII, we report CAP-EOM-EA-CCSD results for the resonance positions and widths of both π^* resonances of 1,3-butadiene. For technical reasons, we employed the aug-cc-pVDZ+3s3p3d(C) basis instead of the aug-cc-pVTZ+3s3p3d(C) basis for this molecule, but in order to test again the validity of the "C" as compared to the "A" scheme, results obtained with the larger aug-cc-pVDZ+3s3p3d(A) basis are also included in Table XIII. Optimal CAP strengths corresponding to the results for the ^2A_u state in Table XIII are 0.0074 a.u, 0.0115 a.u., and 0.0210 a.u. for the zeroth-order and first-order CAP-EOM-EA-CCSD calculations with the "C" basis-set and 0.0135 a.u., 0.0175 a.u., and 0.0310 a.u. for the respective calculations with the "A" basis set. For the ^2B_g state, optimal CAP strengths of 0.0098 a.u., 0.0270 a.u., and 0.0190 a.u. were obtained with the "C" basis set and of 0.0165 a.u., 0.0170 a.u., and 0.0350 a.u. with the "A" basis set.

Table XIII illustrates that aug-cc-pVDZ+3s3p3d(C) and aug-cc-pVDZ+3s3p3d(A) yield very similar results for the resonance position. CAP-EOM-EA-CCSD overestimates the position of the ^2A_u resonance by about 0.7 eV regardless of the basis set used and also independent of whether the first-order correction is applied. For the ^2B_g state an overall better agreement with experiment is found (0.2-0.3 eV), but the first-order correction makes a sizable impact and moves the CAP-EOM-EA-CCSD values away from the experimental value. Note that based on the findings from Section IV, one should expect a significant change of all results when increasing the valence basis set.

Concerning the resonance width, our results support the experiment's hypothesis that the ^2A_u state is considerably longer lived than the ^2B_g state. We also note that first-order results for the resonance width are smaller by 0.05 eV for the ^2A_u state and by 0.2-0.3 eV for the ^2B_g state. Also, the change from the "C" to the "A" basis set makes an impact of

similar magnitude but in opposite direction. A final judgment of the accuracy of the results, however, cannot be made due to the lack of other theoretical or experimental estimates for the resonance width.

VI. CONCLUSIONS

A complete and robust implementation of CAPs within EOM-EE-CCSD and EOM-EA-CCSD methods has been presented together with a protocol for studying molecular shape resonances without system-dependent optimization of basis set and CAP parameters.

In our approach, we have chosen the onset of the CAP as the expectation value of the spatial extent of the reference-state wave function, which ensures that the ground state is minimally perturbed by the CAP ($\sim 10^{-5}$ a.u.). We showed that resonance positions and lifetimes obtained from energies, which are corrected for the CAP perturbation in first order [16, 24], are less sensitive (~ 0.03 eV) towards variation of the CAP onset than uncorrected zeroth-order energies. To determine the optimal CAP strength, we used the criterion from Ref. [24] for the separate stabilization of the real and imaginary part of the first-order corrected energy instead of the most widely used criterion $|\eta\ dE/d\eta| = min$ based on the zeroth-order energy.

Based on benchmark studies for the π^* resonances of CO^- and $C_2H_4^-$, we illustrated that standard valence basis sets (for example, aug-cc-pVTZ) augmented by a set of diffuse functions in the center of the molecule are suitable for the study of resonance states with CAP-EOM-EA-CCSD. We showed that the use of only few diffuse functions of each angular momentum is sufficient for an accurate description of the diffuse part of the resonance wave function. The further addition of diffuse functions has little impact on resonance positions and lifetimes. We also note that the inclusion of diffuse functions with angular momentum up to $\ell = 2$ (d-functions) is essential for π^* resonances, thus suggesting that a set [3s3p3d] of diffuse functions should be sufficient for most applications. The convergence of resonance positions and especially lifetimes with respect to the valence basis set is less clear, which indicates that electron correlation is of higher importance for resonances than for bound states. Although the theoretical understanding of the lifetime's dependence on the valence basis set remains an open problem, we emphasize that we did not observe variations of more than 0.15 eV in the lifetime. Regarding the resonance position, we showed that

the performance of CAP-EOM-EA-CCSD is overall similar to that of EOM-EA-CCSD for bound electron-attached states. In total, our results for a variety of π^* shape resonances demonstrate that CAP-EOM-EA-CCSD is competitive relative to other approaches for the theoretical treatment of resonances and often able to reproduce experimental results for resonance positions and lifetimes. The importance of electron correlation is again illustrated comparing with the results from mean-field approaches, which often disagree qualitatively with experiment.

While the current paper shows the potential of CAP-EOM-CCSD approaches, it is also clear that the application to larger systems is hampered by the need to calculate η-trajectories, i.e., to recalculate the energy for different values of the CAP strength, which increases the computational cost considerably as compared to conventional EOM-CCSD calculations. To make our current implementation of CAP-EOM-CCSD faster and to increase its black-box character, a number of improvements will be pursued in future work. As the wave function changes smoothly with the CAP strength, one can expect that the use of the wave function parameters from the previous step as guess will accelerate the calculation of η-trajectories significantly provided that sufficiently small step sizes are used. A further automatization will be possible by the implementation of analytic derivatives $dE/d\eta$ as this will enable the determination of optimal CAP strengths without that the user has to specify a step size and a range, where the search is performed. Put together, these developments will allow for the application of CAP-EOM-CCSD to resonance states of larger molecules as, for example, biochromophores[139, 140], where standard EOM-CCSD is routinely used for the characterization of bound states.

VII. ACKNOWLEDGMENTS

This work is supported by the Army Research Office through the W911NF-12-1-0543 grant (AIK). We also acknowledge support from the Humboldt Research Foundation (Bessel Award to AIK and Feodor Lynen fellowship to TCJ). MHG, EE, and ES were supported by the Scientific Discovery through Advanced Computing (SciDAC) program funded by the U.S. Department of Energy, Office of Science, Advanced Scientific Computing Research and Basic Energy Sciences. We thank Dr. Y. Sajeev and Prof. Nimrod Moiseyev for helpful comments.

VIII. TABLES

TABLE I: EOM-EE-CCSD excitation energies and expectation values $\langle R^2 \rangle$ for several excited states of CO and C_2H_4 computed using the aug-cc-pVTZ basis set with additional diffuse basis functions placed at the all heavy atoms (A) or at the center of the molecule (C).

		aug-cc-pVTZ + 3s3p3d(A)		aug-cc-pVTZ + 3s3p3d(C)
Molecule	State	$\langle R^2 \rangle$/a.u.[a]	E/eV	E/eV
CO	$2\ ^1A_1$	77.8	10.961	10.961
	$4\ ^1A_1$	153.7	12.559	12.597
	$1\ ^1B_2$	41.4	8.625	8.626
C_2H_4	$2\ ^1A_g$	152.0	8.445	8.446
	$1\ ^1B_{1g}$	116.7	9.791	9.791
	$1\ ^1B_{1u}$	118.7	7.392	7.392

[a]The corresponding values for the ground states are 40.0 a.u. for CO and 83.3 a.u. for C_2H_4.

TABLE II: Dependence of resonance positions E_R and widths Γ of the $^2\Pi$ resonance of CO^- and the $^2B_{2g}$ resonance of $C_2H_4^-$ on the onset of the CAP. Values for η_{opt}, $(\eta \cdot \text{dE}/\text{d}\eta)_{\eta=\eta_{\text{opt}}}$, and $\|W\|$ are also reported. All values computed at the CAP-EOM-EA-CCSD/aug-cc-pVTZ+3s3p3d(C) level of theory.

Relative CAP onset[a]	Zeroth-order values				First-order values				
$\Delta r_x^0/\Delta r_y^0/\Delta r_z^0$/a.u.	E_R/eV	Γ/eV	η_{opt}/a.u.	$\eta\frac{dE}{d\eta}$/a.u.	E_R/eV[b]	Γ/eV[b]	η_{opt}^R/a.u.	η_{opt}^I/a.u.	$\|W\|$/a.u.[c]
CO^-, $^2\Pi$ resonance									
0.0/0.0/0.0	2.088	0.650	0.0028	0.0017	1.981	0.585	0.0054	0.0048	241.9
0.5/0.5/0.0	2.061	0.612	0.0036	0.0021	1.956	0.573	0.0066	0.0060	214.0
-0.5/-0.5/0.0	2.113	0.691	0.0022	0.0011	1.999	0.591	0.0044	0.0040	274.2
0.0/0.0/0.5	2.087	0.644	0.0030	0.0017	1.981	0.582	0.0056	0.0050	235.4
0.0/0.0/-0.5	2.091	0.654	0.0028	0.0015	1.980	0.591	0.0052	0.0046	249.6
$C_2H_4^-$, $^2B_{2g}$ resonance									
0.0/0.0/0.0	2.091	0.430	0.0046	0.0023	2.032	0.328	0.0060	0.0085	272.0
0.5/0.0/0.0	2.089	0.434	0.0045	0.0023	2.032	0.330	0.0054	0.0089	266.7
-0.5/0.0/0.0	2.093	0.427	0.0046	0.0019	2.031	0.328	0.0054	0.0083	278.3
0.0/0.5/0.0	2.095	0.429	0.0050	0.0022	2.033	0.330	0.0057	0.0087	260.5
0.0/-0.5/0.0	2.093	0.431	0.0046	0.0019	2.032	0.326	0.0054	0.0083	285.4
0.0/0.0/0.5	2.088	0.388	0.0071	0.0020	2.023	0.301	0.0070	0.0109	255.3
0.0/0.0/-0.5	2.106	0.478	0.0037	0.0025	2.039	0.353	0.0042	0.0068	291.2

[a] A value of 0.0 refers to $r_\alpha^0 = \sqrt{\langle \alpha^2 \rangle}$, $\alpha = x, y, z$. 0.5/0.5/0.0 means for example that $r_x^0 = \sqrt{\langle x^2 \rangle} + 0.5$, $r_y^0 = \sqrt{\langle y^2 \rangle} + 0.5$, $r_z^0 = \sqrt{\langle z^2 \rangle}$.

[b] Identical to U^R and $-1/2\,U^I$ from Eqs. (7) and (8).

[c] Computed as Frobenius norm.

TABLE III: Resonance positions E_R and widths Γ as well as values for η_{opt} and $\|W\|$ for the $^2\Pi$ resonance of CO^- and the $^2B_{2g}$ resonance of $C_2H_4^-$ computed by CAP-EOM-EA-CCSD using the aug-cc-pVTZ basis set with different additional augmentation. The variations reported for E_R and Γ refer to the change of these quantities upon varying the most important CAP onset parameter by 0.5 a.u. (see Section IV B).

Basis Set	Zeroth-order values			First-order values				
	E_R/eV	Γ/eV	η_{opt}/a.u.	E_R/eV[a]	Γ/eV[a]	η^R_{opt}/a.u.	η^I_{opt}/a.u.	$\|W\|$/a.u.[b]
CO^-, $^2\Pi$ resonance								
aug-cc-pVTZ	2.517 ± 0.013	0.482 ± 0.120	0.0180	—[c]	0.252 ± 0.020	—[c]	0.0660	12.1
aug-cc-pVTZ + 3s(C)	2.517 ± 0.013	0.469 ± 0.120	0.0190	—[c]	0.215 ± 0.021	—[c]	0.0585	49.3
aug-cc-pVTZ + 6s(C)	2.518 ± 0.014	0.468 ± 0.012	0.0190	—[c]	—[c]	—[c]	—[c]	412.0
aug-cc-pVTZ + 3s3p(C)	2.025 ± 0.015	0.549 ± 0.024	0.0024	1.825 ± 0.004	0.357 ± 0.009	0.0082	0.0048	229.5
aug-cc-pVTZ + 6s6p(C)	2.023 ± 0.017	0.551 ± 0.023	0.0024	1.830 ± 0.004	0.364 ± 0.008	0.0082	0.0048	1078.3
aug-cc-pVTZ + 3s3p3d(C)	2.088 ± 0.026	0.650 ± 0.040	0.0028	1.981 ± 0.022	0.585 ± 0.012	0.0054	0.0048	241.9
aug-cc-pVTZ + 6s6p6d(C)	2.112 ± 0.027	0.665 ± 0.055	0.0034	2.015 ± 0.025	0.555 ± 0.057	0.0048	0.0340	1441.8
aug-cc-pVTZ + 3s3p3d3f(C)	2.081 ± 0.028	0.654 ± 0.043	0.0030	1.969 ± 0.022	0.588 ± 0.015	0.0056	0.0050	243.7
aug-cc-pVTZ + 3s3p(A)	2.102 ± 0.024	0.604 ± 0.050	0.0034	1.961 ± 0.016	0.446 ± 0.0026	0.0098	0.0066	505.9
aug-cc-pVTZ + 3s3p3d(A)	2.060 ± 0.022	0.885 ± 0.022	0.0016	1.969 ± 0.025	0.474 ± 0.032	0.0026	0.0305	541.0
$C_2H_4^-$, $^2B_{2g}$ resonance								
aug-cc-pVTZ	2.433[d]	0.479[d]	0.0380	2.411[d]	0.140[d]	0.0880	0.1610	11.8
aug-cc-pVTZ + 3s(C)	2.433[d]	0.479[d]	0.0383	2.411[d]	—[c]	0.0878	—[c]	51.9
aug-cc-pVTZ + 3s3p(C)	2.422 ± 0.024	0.495 ± 0.012	0.0370	2.410 ± 0.007	0.208 ± 0.030	0.1200	0.1700	253.5
aug-cc-pVTZ + 6s6p(C)	2.419[d]	0.494[d]	0.0360	2.409[d]	0.222[d]	0.1250	0.1690	1429.0
aug-cc-pVTZ + 3s3p3d(C)	2.091 ± 0.015	0.430 ± 0.046	0.0046	2.032 ± 0.009	0.328 ± 0.027	0.0060	0.0085	272.0
aug-cc-pVTZ + 6s6p6d(C)	1.976[d]	0.563[d]	0.0013	2.043[d]	0.334[d]	0.0076	0.0100	2014.7
aug-cc-pVTZ + 3s3p3d3f(C)	2.088[d]	0.441[d]	0.0046	2.028[d]	0.334[d]	0.0051	0.0085	274.0
aug-cc-pVTZ + 3s3p(A)	2.108 ± 0.018	0.420 ± 0.045	0.0049	2.017 ± 0.007	0.305 ± 0.030	0.0110	0.0085	502.8
aug-cc-pVTZ + 3s3p3d(A)	2.302 ± 0.043	0.536 ± 0.096	0.0245	2.180 ± 0.008	0.373 ± 0.050	0.0370	0.0290	539.2

[a]Identical to U^R and $-1/2\,U^I$ from Eqs. (7) and (8).

[b]Computed as Frobenius norm.

[c]No stationary point could be located in the range $0 < \eta < 0.2$.

[d]We did not vary the CAP onset in calculations using these basis sets.

TABLE IV: Resonance positions E_R and widths Γ as well as values for η_{opt} for the $^2\Pi$ resonance of CO^- and the $^2B_{2g}$ resonance of $C_2H_4^-$ computed by CAP-EOM-EA-CCSD using different valence basis sets. For comparison purposes, EOM-EE-CCSD excitation energies for several bound states of CO and C_2H_4 are reported as well.

	aug-cc-pVDZ +3s3p3d(C)	aug-cc-pVTZ +3s3p3d(C)	aug-cc-pVQZ +3s3p3d(C)	aug-cc-pV5Z + 3s3p3d(C)
	$^2\Pi$ resonance of CO^-			
E_R (0th order)/eV	2.303	2.088	1.987	1.926
Γ (0th order)/eV	0.727	0.650	0.696	0.804
η_{opt}/a.u.	0.0046	0.0028	0.0020	0.0015
E_R (1st order)/eV[a]	2.182	1.981	1.851	1.762
Γ (1st order)/eV[a]	0.667	0.585	0.673	0.604
η^R_{opt}/a.u.	0.0175	0.0054	0.0062	0.0034
η^I_{opt}/a.u.	0.0100	0.0048	0.0046	0.0028
	Bound states of CO			
E ($2\ ^1A_1$)/eV	10.777	10.961	11.021	11.046
E ($4\ ^1A_1$)/eV	12.446	12.597	12.642	12.663
E ($1\ ^1B_2$)/eV	8.703	8.626	8.612	8.608
	$^2B_{2g}$ resonance of $C_2H_4^-$			
E_R (0th order)/eV	2.191	2.091	1.988	—
Γ (0th order)/eV	0.436	0.430	0.447	—
η_{opt}/a.u.	0.0032	0.0046	0.0025	—
E_R (1st order)/eV[a]	2.230	2.032	1.903	—
Γ (1st order)/eV[a]	0.302	0.328	0.373	—
η^R_{opt}/a.u.	0.0210	0.0060	0.0054	—
η^I_{opt}/a.u.	0.0248	0.0085	0.0043	—
	Bound states of C_2H_4			
E ($2\ ^1A_g$)/eV	8.315	8.446	8.493	—
E ($1\ ^1B_{1g}$)/eV	9.681	9.791	9.830	—
E ($1\ ^1B_{1u}$)/eV	7.279	7.392	7.436	—

[a]Identical to U^R and $-1/2\,U^I$ from Eqs. (7) and (8).

TABLE V: Energy decomposition analysis for the real and imaginary parts of the energies[a] of the $^2\Pi$ resonance of CO^- and the $^2B_{2g}$ resonance of $C_2H_4^-$ computed by CAP-EOM-EA-CCSD using different valence basis sets. All values in atomic units.

	aug-cc-pVDZ +3s3p3d(C)	aug-cc-pVTZ +3s3p3d(C)	aug-cc-pVQZ +3s3p3d(C)	aug-cc-pV5Z + 3s3p3d(C)
	$^2\Pi$ resonance of CO^-			
Total energy (real)	-112.9835	-113.0979	-113.1573	-113.1805
One-electron part (real)[b]	-112.5652	-112.5920	-112.6078	-112.6167
Two-electron part (real)	-0.4183	-0.5059	-0.5495	-0.5638
Total energy (imaginary)	-0.0136	-0.0121	-0.0129	-0.0148
One-electron part (imaginary)	-0.0479	-0.0485	-0.0559	-0.0725
Two-electron part (imaginary)	0.0343	0.0364	0.0430	0.0577
	$^2B_{2g}$ resonance of $C_2H_4^-$			
Total energy (real)	-78.2836	-78.3881	-78.4333	—
One-electron part (real)[b]	-77.8614	-77.8781	-77.8935	—
Two-electron part (real)	-0.4223	-0.5100	-0.5399	—
Total energy (imaginary)	-0.0080	-0.0080	-0.0082	—
One-electron part (imaginary)	-0.0289	-0.0318	-0.0389	—
Two-electron part (imaginary)	0.0209	0.0238	0.0307	—

[a]Evaluated at the respective η_{opt}, see values in Table IV.

[b]Including nuclear repulsion energy.

TABLE VI: Computational details of CAP-EOM-EA-CCSD calculations on N_2^-, CO^-, $C_2H_2^-$, $C_2H_4^-$, CH_2O^-, CO_2^-, and $C_4H_6^-$.

Molecule (State)	Leading configuration in the real part of the wave function	Bond lengths (in bohr) and angles	Orientation	CAP onset (in bohr) r_x^0	r_y^0	r_z^0
N_2^- $(1\ ^2\Pi_g)$	$(1\sigma_g)^2(1\sigma_u)^2(2\sigma_g)^2(2\sigma_u)^2$ $(3\sigma_g)^2(1\pi_u)^4(1\pi_g)^1$	R(NN) = 2.0740	z-axis = molecular axis	2.76	2.76	4.88
CO^- $(1\ ^2\Pi)$	$(1\sigma)^2(2\sigma)^2(3\sigma)^2(4\sigma)^2$ $(5\sigma)^2(1\pi)^4(2\pi)^1$	R(CO) = 2.1316	z-axis = molecular axis	2.76	2.76	4.97
$C_2H_2^-$ $(1\ ^2\Pi_g)$	$(1\sigma_g)^2(1\sigma_u)^2(2\sigma_g)^2(2\sigma_u)^2$ $(3\sigma_g)^2(1\pi_u)^4(1\pi_g)^1$	R(CC) = 2.2733 R(CH) = 2.0088	z-axis = molecular axis	3.20	3.20	6.35
$C_2H_4^-$ $(1\ ^2B_{2g})$	$(1a_g)^2(1b_{1u})^2(2a_g)^2(2b_{1u})^2$ $(1b_{2u})^2(3a_g)^2(1b_{3g})^2(1b_{3u})^2(1b_{2g})^1$	R(CC) = 2.5303 R(CH) = 2.0522 $\angle$(CCH) = 121.2°	z-axis $\perp$ molecular plane x-axis = CC bond	7.10	4.65	3.40
CH_2O^- $(1\ ^2B_1)$	$(1a_1)^2(2a_1)^2(3a_1)^2(4a_1)^2$ $(1b_2)^2(5a_1)^2(1b_1)^2(2b_2)^2(2b_1)^1$	R(CO) = 2.2771 R(CH) = 2.0995 $\angle$(HCO) = 121.9°	z-axis = CO bond y-axis $\perp$ molecular plane	3.85	2.95	6.10
CO_2^- $(1\ ^2\Pi_u)$	$(1\sigma_g)^2(1\sigma_u)^2(2\sigma_g)^2(2\sigma_u)^2(3\sigma_g)^2$ $1(\pi_u)^4(3\sigma_u)^2(4\sigma_g)^2(1\pi_g)^4(2\pi_u)^1$	R(CO) = 2.1978	z-axis = molecular axis	3.33	3.33	9.57
$C_4H_6^-$ $(1\ ^2A_u)$ $(1\ ^2B_g)$	(core)$^2(6b_u)^2(7a_g)^2(1a_u)^2(1b_g)^2(2a_u)^1$ [a] (core)$^2(6b_u)^2(7a_g)^2(1a_u)^2(1b_g)^2(2b_g)^1$ [a]	see footnote[b]		16.20	7.25	4.65

[a] (core)$^2 = (1b_u)^2(1a_g)^2(2b_u)^2(2a_g)^2(3a_g)^2(3b_u)^2(4a_g)^2(4b_u)^2(5b_u)^2(5a_g)^2(6a_g)^2$

[b] Cartesian coordinates of symmetry-unique nuclei are in bohr: C(1.15735915, 0.76277974, 0.0), C(3.48113356, -0.22898634, 0.0), H(0.92483778, 2.80751355, 0.0), H(3.78431564, -2.26062161, 0.0), H(5.15268958, 0.95838430, 0.0)

TABLE VII: Resonance positions E_R and widths Γ for the $^2\Pi_g$ resonance state of N_2^- obtained using different methods.

Method	E_R/eV	Γ/eV
Stieltjes imaging technique/special basis set[a]	2.23	0.40
Schwinger variational method/ADC(3)/(11s8p3d)/[5s7p3d][b]	2.534	0.536
Complex scaling/HF-SCF/Dunning's (9s5p)/[5s3p]+2d+(5p2d)/[3p2d]+4p6d[c]	3.19	0.44
Complex scaling/MR-CI/Dunning's (9s5p)/[5s3p]+1d+10p[d]	1.38	0.414
Complex scaling/Σ^3 decouplings of the e^--propagator/[4s9p][e]	2.11	0.18
Stabilization/MR-CI/ Dunning's (9s5p)/[5s3p]+3p2d+4s1p1d(C)[f]	2.62	0.45
Stabilization/MR-CI/6-31+G*+3p[g]	2.34	0.51
Stabilization/MP-PT2/ANO(14s9p4d3f)/[4s3p2d1f]+2s2p7d4g(C)[h]	2.36	0.42
Stabilization/CIS/aug-cc-pVTZ+3p[i]	3.77	1.14
Stabilization/TDDFT(HFE_PBE)/aug-cc-pVTZ+3p[i]	3.078	0.54
Stabilization/EOM-EA-CCSD/aug-cc-pVTZ+3p[i]	2.58	0.570
Stabilization/EOM-EA-CCSD/aug-cc-pVQZ+3p[i]	2.49	0.502
Stabilization/EOM-EA-CCSD/aug-cc-pV5Z+3p[i]	2.49	0.496
CAP/static exchange/[5s10p13d] (0th order)[j]	3.888	1.363
CAP/static exchange/[5s10p13d] (1st order)[j]	3.776	1.199
CAP-HF-SCF/(11s7p2d)/[5s4p2d][k]	3.28	0.395
CAP-DFT(LSD/XC)/(11s7p2d)/[5s4p2d][k]	3.39	0.506
CAP-MRCI/Dunning's (9s5p)/[5s3p]+(12p)/[9p]+2d[l]	2.97	0.65
TCAP-MRCI/Dunning's (11s6p)/[5s3p]+7p3d2f[m]	2.42	0.45
CAP-Σ(ADC(2))/TZP+9p2d2f[n]	2.58	0.55
CAP-FSMRCC/TZ(7p2d)[o]	2.52	0.39
CAP-CIP/TZ(7p2d)[p]	2.28	0.482
CAP-EOM-EA-CCSD/(11s8p3d)/[5s7p3d]+3p[q]	2.07	0.42
CAP-EOM-EA-CCSD/aug-cc-pVTZ+3s3p3d(C) (0th order)[r]	2.487	0.417
CAP-EOM-EA-CCSD/aug-cc-pVTZ+3s3p3d(C) (1st order)[r]	2.571	0.255
CAP-EOM-EA-CCSD/aug-cc-pVQZ+3s3p3d(C) (0th order)[r]	2.508	0.364
CAP-EOM-EA-CCSD/aug-cc-pVQZ+3s3p3d(C) (1st order)[r]	2.478	0.286
Estimate via Feshbach projection formalism based on experimental data[s]	2.32	0.41

[a] See Ref. [83].
[b] See Ref. [84].
[c] See Ref. [81].
[d] See Ref. [10].
[e] See Ref. [82].
[f] See Ref. [69].
[g] See Ref. [79].
[h] See Ref. [70].
[i] See Ref. [80].
[j] See Ref. [16].
[k] See Ref. [27].
[l] See Ref. [63].
[m] See Ref. [62].
[n] See Ref. [64].
[o] See Ref. [65].
[p] See Ref. [66].
[q] See Ref. [26].
[r] This work.
[s] See Ref. [89].

TABLE VIII: Resonance positions E_R and widths Γ for the $^2\Pi$ resonance state of CO^- obtained using different methods.

Method	E_R/eV	Γ/eV
Boomerang model[a]	1.52	0.80
Close coupling method[b]	1.75	0.28
T-matrix/static exchange/(9s5p1d)/[4s3p1d][c]	3.4	1.65
Complex scaling/Σ^2 decouplings of the e^- propagator (real SCF)/4s5p[d]	1.71	0.08
Complex scaling/Σ^3 decouplings of the e^- propagator/4s5p[e]	1.65	0.14
Stabilization/MP-PT2/ANO(14s9p4d3f)/[4s3p2d1f]+2s4p7d5f(C)[f]	2.02	0.35
CAP-EOM-EA-CCSD/4s5p(C)+4s5p1d(O)[g]	1.32	0.12
CAP-EOM-EA-CCSD/maug-cc-pV(D+d)Z+3p[g]	1.42	0.44
CAP-EOM-EA-CCSD/aug-cc-pVTZ+3s3p(A) (1st order)[h]	1.954	0.433
CAP-EOM-EA-CCSD/aug-cc-pVTZ+3s3p3d(C) (0th order)[i]	2.088	0.650
CAP-EOM-EA-CCSD/aug-cc-pVTZ+3s3p3d(C) (1st order)[i]	1.981	0.585
CAP-EOM-EA-CCSD/aug-cc-pV5Z+3s3p3d(C) (0th order)[i]	1.926	0.804
CAP-EOM-EA-CCSD/aug-cc-pV5Z+3s3p3d(C) (1st order)[i]	1.762	0.604
Experiment[j]	1.50	0.40

[a]See Ref. [90].
[b]See Ref. [91].
[c]See Ref. [92].
[d]See Ref. [93].
[e]See Ref. [82].
[f]See Ref. [70].
[g]See Ref. [26].
[h]See Ref. [24].
[i]This work.
[j]See Ref. [94].

TABLE IX: Resonance positions E_R and widths Γ for the $^2\Pi_g$ resonance state of $C_2H_2^-$ obtained using different methods.

Method	E_R/eV	Γ/eV
Theory		
Multiple scattering Xα[a]	2.6	1.0
Feshbach projection/MR-CI/Dunning's (9s5p)/[5s3p]+1p1d+3p[b]	2.96	1.11
Complex scaling/Σ^3 decouplings of the e^--propagator/5s9p1d, 3s3p(H)[c]	2.50	0.21
Stabilization method/EOM-EA-CCSD/aug-cc-pVTZ+3p[d]	2.77	1.50
Stabilization method/TDDFT(HFE_PBE)/aug-cc-pVTZ+3p[d]	2.4	0.6
CAP-EOM-EA-CCSD/Dunning's (9s5p)/[5s3p]+4p1d(C), 2s1p(H)[e]	1.79	0.80
CAP-EOM-EA-CCSD/aug-cc-pVTZ+3s3p3d(C) (0th order)[f]	2.655	0.979
CAP-EOM-EA-CCSD/aug-cc-pVTZ+3s3p3d(C) (1st order)[f]	2.450	0.831
Experiment		
Trapped electron[g]	1.80/1.85	—
Vibrational excitation[h]	2.6	>1.0
Electron impact[i]	2.5	—
Dissociative attachment/electron transmission[j]	2.6	—
Electron transmission[k]	2.6	∼0.8

[a]See Ref. [95].
[b]See Ref. [96].
[c]See Ref. [82].
[d]See Ref. [80].
[e]See Ref. [26].
[f]This work.
[g]See Refs. [98] and [103].
[h]See Ref. [100].
[i]See Ref. [101].
[j]See Ref. [102].
[k]See Ref. [99].

TABLE X: Resonance positions E_R and widths Γ for the $^2B_{2g}$ resonance state of $C_2H_4^-$ obtained using different methods.

Method	E_R/eV	Γ/eV
Theory		
Complex scaling/second order rotated propagator/5s7p[a]	1.94	0.110
Complex scaling/second order rotated propagator/5s8p[a]	2.49	0.234
Complex scaling/second order rotated propagator/5s9p[a]	1.88	0.442
Complex Kohn method[b]	1.83	0.460
Complex scaling/bi-variational SCF/5s7p [c]	1.93	0.2
Complex scaling/ Second order biorthogonal e^- propagator/5s7p[d]	1.86	0.18
Complex scaling/ Diagonal 2ph-TDA biorthogonal e^- propagator/5s7p[d]	1.89	0.18
Stabilization method/EOM-CCSD/aug-cc-pVTZ+3p[e]	2.06	0.64
Stabilization method/EOM-MP2/aug-cc-pVTZ+3p[e]	1.91	0.60
Stabilization method/ADC(2)/aug-cc-pVTZ+3p[e]	1.78	0.49
Stabilization method/Koopmans theorem (HFE_BLYP)/aug-cc-pVTZ+3p[e]	2.58	1.32
Stabilization method/Koopmans theorem (HFE_BPE)/aug-cc-pVTZ+3p[e]	2.62	1.08
Stabilization method/TDDFT (HFE_BPE)/aug-cc-pVTZ+3p[e]	2.49	0.31
CAP-CIP-$V_c^{(1,0)}(\eta^2)$/5s9p[f]	1.778	0.9076
CAP-FSMRCC-$V_c^{(1,0)}(\eta^2)$/aug-cc-pVDZ[g]	1.802	0.3662
CAP-EOM-EA-CCSD/aug-cc-pVTZ+3s3p3d(C) (0th order) [h]	2.091	0.430
CAP-EOM-EA-CCSD/aug-cc-pVTZ+3s3p3d(C) (1st order) [h]	2.032	0.328
CAP-EOM-EA-CCSD/aug-cc-pVQZ+3s3p3d(C) (0th order) [h]	1.988	0.447
CAP-EOM-EA-CCSD/aug-cc-pVQZ+3s3p3d(C) (1st order) [h]	1.903	0.373
Experiment		
Electron scattering[i]	1.78	—
Electron impact[j]	1.8	0.7
Elastic scattering[k]	1.8	0.7

[a]See Ref. [107].
[b]See Ref. [108].
[c]See Ref. [109].
[d]See Ref. [110].
[e]See Ref. [80].
[f]See Ref. [66].
[g]See Ref. [67].
[h]This work.
[i]See Ref. [104], vertical electron affinity used.
[j]See Ref. [105].
[k]See Ref. [106].

TABLE XI: Resonance positions E_R and widths Γ for the $^2B_1$ resonance state of CH_2O^- obtained using different methods.

Method	E_R/eV	Γ/eV
Theory		
Complex Kohn method[a]	1.0	0.5
Static exchange[a]	3.0	—
Complex scaling/zeroth-order e^- propagator/4s6p1d(C)/2s1p(H)[b]	1.0	0.1
Complex scaling/quasiparticle second-order e^- propagator/4s6p1d(C)/2s1p(H)[b]	0.99	0.1
Complex scaling/diagonal 2ph-TDA e^- propagator/4s6p1d(C)/2s1p(H)[b]	0.89	0.12
R-matrix method/augmented DZP[c]	1.32	0.546
R-matrix method/DZP[d]	1.46	0.794
Finite-element-discrete-model method[e]	0.682	0.429
CAP-SAC-CI /cc-pVDZ+[2s5p2d/2s2p] [f]	1.219	0.488
CAP-SAC-CI /cc-pVTZ+[2s5p2d/2s2p] [f]	1.119	0.462
CAP-SAC-CI /cc-pVQZ+[2s5p2d/2s2p] [f]	1.094	0.418
CAP-EOM-EA-CCSD/aug-cc-pVTZ+3s3p3d(C) (0th order)[g]	1.352	0.376
CAP-EOM-EA-CCSD/aug-cc-pVTZ+3s3p3d(C) (1st order)[g]	1.314	0.277
Experiment		
Electron transmission spectroscopy[h]	0.86	—
Vibrational excitation[i]	0.87	—

[a]See Ref. [115, 116].
[b]See Ref. [117].
[c]See Ref. [118].
[d]See Ref. [119].
[e]See Ref. [120].
[f]See Ref. [25].
[g]This work.
[h]See Ref. [111, 112].
[i]See Ref. [113].

TABLE XII: Resonance positions E_R and widths Γ for the $^2\Pi_u$ resonance state of CO_2^- obtained using different methods.

Method	E_R/eV	Γ/eV
Theory		
Scattering/static exchange+polarization/DZP basis set[a]	3.8	0.5
Schwinger variational method/static exchange/[5p4d/5p4d1f][b]	5.39	0.64
Schwinger variational method/static exchange+polarization/[5s3p]+4s3p3d[c]	3.78	0.23
Close coupling/static exchange+polarization/DZP+add. diffuse functions[d]	3.88	0.34
CAP-EOM-EA-CCSD/aug-cc-pVTZ+3s3p3d(C) (0th order)[e]	4.020	0.119
CAP-EOM-EA-CCSD/aug-cc-pVTZ+3s3p3d(C) (1st order)[e]	3.997	0.198
Experiment		
Electron scattering[f]	3.8	–
Electron transmission spectroscopy[g]	3.14[h]	0.20 ± 0.07
Electron impact[i]	3.8	–
Impact of slow electrons[j]	3.6	–
Electron transmission spectroscopy[k]	3.58	–
High resolution attachment spectrometry[l]	4.4	–

[a]See Ref. [133].
[b]See Ref. [134].
[c]See Ref. [135].
[d]See Ref. [136].
[e]This work.
[f]See Ref. [121].
[g]See Refs. [122, 126].
[h]The energy of the lowest observed vibrational level is given.
[i]See Ref. [123].
[j]See Ref. [124].
[k]See Ref. [125].
[l]See Ref. [127].

TABLE XIII: Resonance positions E_R and widths Γ for the ^2A_u and ^2B_g resonance states of $C_4H_6^-$ (1,3-butadiene anion) obtained using different methods.

Method	E_R/eV	Γ/eV
^2A_u state		
Theory		
DFT/B3-LYP/6-311+G(2df,p)[a]	0.76	–
CAP-EOM-EA-CCSD/aug-cc-pVDZ+3s3p3d(C) (0th order)[b]	1.336	0.110
CAP-EOM-EA-CCSD/aug-cc-pVDZ+3s3p3d(C) (1st order)[b]	1.327	0.059
CAP-EOM-EA-CCSD/aug-cc-pVDZ+3s3p3d(A) (0th order)[b]	1.348	0.145
CAP-EOM-EA-CCSD/aug-cc-pVDZ+3s3p3d(A) (1st order)[b]	1.332	0.103
Experiment[c]	0.62	–
^2B_g state		
Theory		
CAP-EOM-EA-CCSD/aug-cc-pVDZ+3s3p3d(C) (0th order)[b]	2.683	0.720
CAP-EOM-EA-CCSD/aug-cc-pVDZ+3s3p3d(C) (1st order)[b]	2.538	0.509
CAP-EOM-EA-CCSD/aug-cc-pVDZ+3s3p3d(A) (0th order)[b]	2.647	0.919
CAP-EOM-EA-CCSD/aug-cc-pVDZ+3s3p3d(A) (1st order)[b]	2.544	0.630
Experiment[c]	2.82	–

[a]See Ref. [138].
[b]This work.
[c]See Ref. [104].

IX. FIGURES

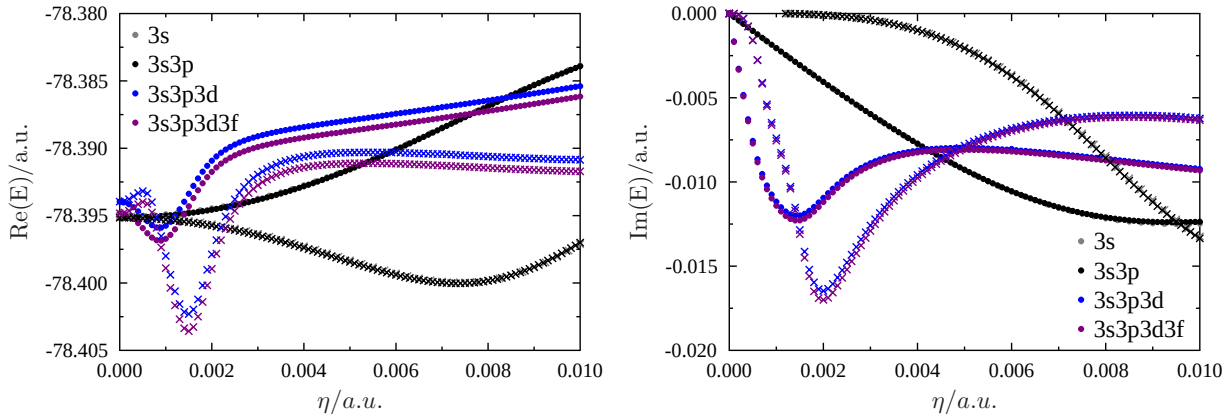

FIG. 1: Real (right) and imaginary (left) parts of E and U as a function of the CAP strength parameter η for the $^2\Pi_g$ resonance of C_2H_4. All values computed by CAP-EOM-EA-CCSD/aug-cc-pVTZ with different additional diffuse functions. • refers to zeroth-order values, × to first-order values.

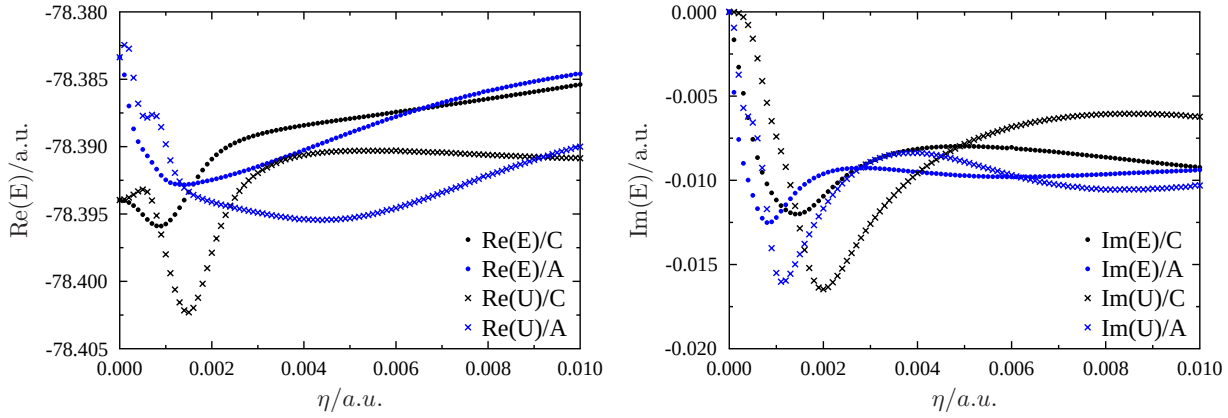

FIG. 2: Real (right) and imaginary (left) parts of E and U as a function of the CAP strength parameter η for the $^2\Pi_g$ resonance of C_2H_4. All values computed by CAP-EOM-EA-CCSD/aug-cc-pVTZ+3s3p3d(C) and aug-cc-pVTZ+3s3p3d(A), respectively. • refers to zeroth-order values, × to first-order values.

X. REFERENCES

[1] S. Klaiman and I. Gilary, Adv. Quantum Chem. **63**, 1 (2012).

[2] W. P. Reinhardt, Annu. Rev. Phys. Chem. **33**, 223 (1982).

[3] N. Moiseyev, Phys. Rep. **302**, 212 (1998).

[4] N. Moiseyev, *Non-Hermitian quantum mechanics*. Cambridge University Press, 2011.

[5] H. Feshbach, Ann. Phys. (N.Y.) **19**, 287 (1962).

[6] J. Aguilar and J. M. Combes, Commun. Math. Phys. **22**, 269 (1971).

[7] T.N. Rescigno, C.W. McCurdy, and A.E. Orel, Phys. Rev. A **17**, 1931 (1978).

[8] D.T. Chuljian and J. Simons, Int. J. Quant. Chem. **XXIII**, 1723 (1983).

[9] P.R. Zdanska and N. Moiseyev, J. Chem. Phys. **123**, 194105 (2005).

[10] M. Honigmann, R. J. Buenker, and H.-P. Liebermann, J. Chem. Phys. **125**, 234304 (2006).

[11] K.B. Bravaya, D. Zuev, E. Epifanovsky, and A.I. Krylov, J. Chem. Phys. **138**, 124106 (2013).

[12] C.W. McCurdy and T.N. Rescigno, Phys. Rev. Lett. **41**, 1364 (1978).

[13] C.W. McCurdy, Phys. Rev. A **21**, 464 (1980).

[14] C. W. McCurdy and T. N. Rescigno, Phys. Rev. A **21**, 1499 (1980).

[15] P. Balanarayan, Y. Sajeev Y., and N. Moiseyev, Chem. Phys. Lett. **524**, 84 (2012).

[16] U. V. Riss and H.-D. Meyer, J. Phys. B **26**, 4503 (1993).

[17] R. Santra and L.S. Cederbaum, Phys. Rep. **368**, 1 (2002).

[18] J.G. Muga, J.P. Palao, B. Navarro, and I.L. Egusquiza, Phys. Rep. **395**, 357 (2004).

[19] U.V. Riss and H.-D. Meyer, J. Phys. B **28**, 1475 (1995).

[20] N. Lipkin, N. Moiseyev, and E. Brändas, Phys. Rev. A **40**, 549 (1989).

[21] C.W. McCurdy, T.N. Rescigno, and D. Byrum, Phys. Rev. A **56**, 1958 (1997).

[22] U.V. Riss and H.-D. Meyer, J. Phys. B **31**, 2279 (1998).

[23] N. Moiseyev, J. Phys. B **31**, 1431 (1998).

[24] T.-C. Jagau, K.B. Bravaya D. Zuev, E. Epifanovsky, and A.I. Krylov, J. Phys. Chem. Lett. **5**, 310 (2014).

[25] M. Ehara and T. Sommerfeld, Chem. Phys. Lett. **537**, 107 (2012).

[26] A. Ghosh, N. Vaval, and S. Pal, J. Chem. Phys. **136**, 234110 (2012).

[27] Y. Zhou and M. Ernzerhof, J. Phys. Chem. Lett. **3**, 1916 (2012).

[28] R. Lefebvre, M. Sindelka, and N. Moiseyev, Phys. Rev. A **72**, 052704 (2005).

[29] R. Lefebvre and N. Moiseyev, J. Phys. B **43**, 095401 (2010).

[30] T. Helgaker, P. Jørgensen, and J. Olsen, *Molecular electronic structure theory*. Wiley & Sons, 2000.

[31] R.J. Bartlett and M. Musial, Rev. Mod. Phys. **79**, 291 (2007).

[32] R.J. Bartlett, Mol. Phys. **108**, 2905 (2010).

[33] A.I. Krylov, Annu. Rev. Phys. Chem. **59**, 433 (2008).

[34] K. Sneskov and O. Christiansen, Wiley Interdisciplinary Reviews: Computational Molecular Science **2**, 566 (2011).

[35] R.J. Bartlett, Wiley Interdisciplinary Reviews: Computational Molecular Science **2**, 126 (2012).

[36] J.A. Pople, Theoretical models for chemistry, in *Energy, Structure and Reactivity: Proceedings of the 1972 Boulder Summer Research Conference on Theoretical Chemistry*, edited by D.W. Smith and W.B. McRae, pages 51–61. Wiley, New York, 1973.

[37] R.J. Bartlett, Int. J. Mol. Sci. **3**, 579 (2002).

[38] T. Sommerfeld and H.-D. Meyer, J. Phys. B **35**, 1841 (2002).

[39] Y. Sajeev, M. Sindelka, and N. Moiseyev, Chem. Phys. **329**, 307 (2006).

[40] Y. Sajeev and N. Moiseyev, J. Chem. Phys. **127**, 034105 (2007).

[41] Y. Sajeev, V. Vysotskiy, L.S. Cederbaum, and N. Moiseyev, J. Chem. Phys. **131**, 211102 (2009).

[42] N. Moiseyev, P.R. Certain, and F. Weinhold, Mol. Phys. **36**, 1613 (1978).

[43] J. Cizek, J. Chem. Phys. **45**, 4256 (1966).

[44] J.A. Pople, R. Krishnan, H.B. Schlegel, and J.S. Binkley, Int. J. Quant. Chem. **14**, 545 (1978).

[45] G.D. Purvis and R.J. Bartlett, J. Chem. Phys. **76**, 1910 (1982).

[46] H. Sekino and R.J. Bartlett, Int. J. Quant. Chem. Symp. **26**, 255 (1984).

[47] J.F. Stanton and R.J. Bartlett, J. Chem. Phys. **98**, 7029 (1993).

[48] M. Head-Gordon and T.J. Lee, in *Modern Ideas in Coupled Cluster Theory*, edited by R.J. Bartlett. World Scientific, Singapore, 1997.

[49] J. Simons, *Encyclopedia of computational chemistry*, chapter Equation of motion (EOM)

methods for computing electron affinities. J. Wiley & Son, New York, 1998.

[50] M. Nooijen and R.J. Bartlett, J. Chem. Phys. **102**, 3629 (1995).

[51] S.V. Levchenko, T. Wang, and A.I. Krylov, J. Chem. Phys. **122**, 224106 (2005).

[52] T. Sommerfeld and F. Tarantelli, J. Chem. Phys. **112**, 2106 (2000).

[53] D. Zuev, K.B. Bravaya, T.D. Crawford, R. Lindh, and A.I. Krylov, J. Chem. Phys. **134**, 034310 (2011).

[54] A.I. Krylov and P.M.W. Gill, WIREs Comput. Mol. Sci. **3**, 317 (2013).

[55] Y. Shao, L. Fusti-Molnar, Y. Jung, J. Kussmann, C. Ochsenfeld, S. Brown, A.T.B. Gilbert, L.V. Slipchenko, S.V. Levchenko, D.P. O'Neill, R.A. Distasio Jr, R.C. Lochan, T. Wang, G.J.O. Beran, N.A. Besley, J.M. Herbert, C.Y. Lin, T. Van Voorhis, S.H. Chien, A. Sodt, R.P. Steele, V.A. Rassolov, P. Maslen, P.P. Korambath, R.D. Adamson, B. Austin, J. Baker, E.F.C. Byrd, H. Daschel, R.J. Doerksen, A. Dreuw, B.D. Dunietz, A.D. Dutoi, T.R. Furlani, S.R. Gwaltney, A. Heyden, S. Hirata, C.-P. Hsu, G.S. Kedziora, R.Z. Khalliulin, P. Klunziger, A.M. Lee, W.Z. Liang, I. Lotan, N. Nair, B. Peters, E.I. Proynov, P.A. Pieniazek, Y.M. Rhee, J. Ritchie, E. Rosta, C.D. Sherrill, A.C. Simmonett, J.E. Subotnik, H.L. Woodcock III, W. Zhang, A.T. Bell, A.K. Chakraborty, D.M. Chipman, F.J. Keil, A. Warshel, W.J. Hehre, H.F. Schaefer III, J. Kong, A.I. Krylov, P.M.W. Gill, M. Head-Gordon, Phys. Chem. Chem. Phys. **8**, 3172 (2006).

[56] E. Epifanovsky, M. Wormit, T. Kuś, A. Landau, D. Zuev, K. Khistyaev, P. Manohar, I. Kaliman, A. Dreuw, and A.I. Krylov, J. Comput. Chem. **34**, 2293 (2013).

[57] A library consisting of a polymorphic orbital class with derived types: RHF, CAP-RHF, restricted open-shell HF, generalized HF, etc., containing the methods which act on the orbitals. These orbital classes couple to a polymorphic nonlinear optimizer class with derived types: steepest descent, direct inversion in the iterative subspace (DIIS), Broyden-Fletcher-Goldfarb-Shanno (BFGS), etc. which calls methods overridden in the derived orbital classes and provides a uniform interface. This design allows for quick prototyping of new orbital classes as each optimizer only requires a limited number of methods. It also allows for code reuse between optimizers such as steepest descent and BFGS.

[58] C. Sanderson, Armadillo: An open source C++ linear algebra library for fast prototyping and computationally intensive experiments, 2010, NICT.

[59] P. Pulay, Chem. Phys. Lett. **73**, 393 (1980).

[60] E.R. Davidson, J. Comput. Phys. **17**, 87 (1975).

[61] A. D. Becke, J. Chem. Phys. **88**, 2547 (1988).

[62] T. Sommerfeld, U. V. Riss, H.-D. Meyer, L. S. Cederbaum, B. Engels, and H. U. Suter, J. Phys. B **31**, 4107 (1998).

[63] T. Sommerfeld and R. Santra, Int. J. Quant. Chem. **82**, 218 (2001).

[64] S. Feuerbacher, T. Sommerfeld, R. Santra, and L. S. Cederbaum, J. Chem. Phys. **118**, 6188 (2003).

[65] Y. Sajeev, R. Santra, and S. Pal, J. Chem. Phys. **122**, 234320 (2005).

[66] Y. Sajeev, R. Santra, and S. Pal, J. Chem. Phys. **123**, (2005).

[67] S. Pal, Y. Sajeev, and N. Vaval, Chem. Phys. **329**, 283 (2006).

[68] R.A. Kendall, Jr. T.H. Dunning, and R.J. Harrison, J. Chem. Phys. **96**, 6796 (1992).

[69] B. M. Nestmann and S. D. Peyerimhoff, J. Phys. B **18**, 4309 (1985).

[70] A. F. Izmaylov, S. O. Adamson, and A. Zaitsevskii, J. Phys. B **37**, 2321 (2004).

[71] C. Ramsauer and R. Kollath, Ann. Phys. **402**, 143 (1931).

[72] G. J. Schulz, Phys. Rev. **125**, 229 (1962).

[73] G. J . Schulz, Phys. Rev. **135**, A988 (1964).

[74] H. G. M. Heideman, C. E. Kuyatt, and G. E. Chamberlain, J. Chem. Phys. **44**, 355 (1966).

[75] D. E. Golden, Phys. Rev. Lett. **17**, 847 (1966).

[76] H. Ehrhardt and K. Willmann, Z. Phys. **204**, 462 (1967).

[77] R. E. Kennerly, Phys. Rev. A **21**, 1876 (1980).

[78] G. J. Schulz, Rev. Mod. Phys. **45**, 423 (1973).

[79] J. S.-Y. Chao, M. F. Falcetta, and K. D. Jordan, J. Chem. Phys. **93**, 1125 (1990).

[80] M. F. Falcetta, L. A. Di Falco, D. S. Ackerman, J. C. Barlow, and K. D. Jordan, J. Phys. Chem. A , DOI: 10.1021/jp5003287 (2014).

[81] T. N. Rescigno, A. E. Orel, and C. W. McCurdy, J. Chem. Phys. **73**, 6347 (1980).

[82] S. Mahalakshmi, A. Venkatnathan, and M. K. Mishra, J. Chem. Phys. **115**, 4549 (2001).

[83] A. U. Hazi, T. N. Rescigno, and M. Kurilla, Phys. Rev. A **23**, 1089 (1981).

[84] H.-D. Meyer, Phys. Rev. A **40**, 5605 (1989).

[85] L. Dubé and A. Herzenberg, Phys. Rev. A **20**, 194 (1979).

[86] J. G. Lauderdale, C. W. McCurdy, and A. U. Hazi, J. Chem. Phys. **79**, 2200 (1983).

[87] A. Ghosh, A. Karne, S. Pal, and N. Vaval, Phys. Chem. Chem. Phys. **15**, 17915 (2013).

[88] M. Honigmann, R. J. Buenker, and H.-P. Liebermann, J. Chem. Phys. **131**, (2009).

[89] M. Berman, H. Estrada, L. S. Cederbaum, and W. Domcke, Phys. Rev. A **28**, 1363 (1983).

[90] M. Zubek and C. Szmytkowski, J. Phys. B **10**, L27 (1977).

[91] N. Chandra, Phys. Rev. A **16**, 80 (1977).

[92] D. A. Levin, A. W. Fliflet, and V. McKoy, Phys. Rev. A **21**, 1202 (1980).

[93] R. A. Donnelly, Int. J. Quant. Chem. **19**, 363 (1986).

[94] H. Erhardt, L. Langhans, F. Linder, and H. S. Taylor, Phys. Rev. **173**, 222 (1968).

[95] J. A. Tossell, J. Phys. B **18**, 387 (1985).

[96] V. Krumbach, B. M. Nestmann, and S. D. Peyerimhoff, J. Phys. B **22**, 4001 (1989).

[97] A. Venkatnathan and M. K. Mishra, Chem. Phys. Lett. **296**, 223 (1998).

[98] D.F. Dance and I. C. Walker, Chem. Phys. Lett. **18**, 601 (1973).

[99] K. D. Jordan and P. D. Burrow, Acc. Chem. Res. **11**, 341 (1978).

[100] K.-H. Kochem, W. Sohn, K. Jung, H. Ehrhardt, and E. S. Chang, J. Phys. B **18**, 1253 (1985).

[101] L. Andric and R. I. Hall, J. Phys. B **21**, 355 (1988).

[102] R. Dressler and M. Allan, J. Chem. Phys. **87**, 4510 (1987).

[103] E. H. van Veen and F. L. Plantenga, Chem. Phys. Lett. **38**, 493 (1976).

[104] P. D. Burrow and K. D. Jordan, Chem. Phys. Lett. **36**, 595 (1975).

[105] I. C. Walker, A. Stamatovic, and S. F. Wong, J. Chem. Phys. **69**, 5532 (1978).

[106] R. Panajotovic, M. Kitajima, H. Tanaka, M. Jelisavcic, J. Lower, L. Campbell, M. J. Brunger, and S. J. Buckman, J. Phys. B **36**, 1615 (2003).

[107] R. A. Donelly, J. Chem. Phys. **84**, 6200 (1986).

[108] B. I. Schneider, T. N. Rescigno, B. H. Lengsfield III, and C. W. McCurdy, Phys. Rev. Lett. **66**, 2728 (1991).

[109] M. N. Medikeri and M. K. Mishra, Chem. Phys. Lett. **246**, 26 (1995).

[110] M. N. Medikeri and M. K. Mishra, J. Chem. Phys. **103**, 676 (1995).

[111] P. D. Burrow and J. A. Michejda, Chem. Phys. Lett. **42**, 223 (1976).

[112] E. H. Van Veen, W. L. Van Dijk, and H. H. Brongersma, Chem. Phys. **16**, 337 (1976).

[113] C. Benoit and R. Abouaf, Chem. Phys. Lett. **123**, 134 (1986).

[114] D. C. Moule and A. D. Walsh, Chem. Rev. **75**, 67 (1975).

[115] T. N. Rescigno, C. W. McCurdy, and B. I. Schneider, Phys. Rev. Lett. **63**, 248 (1989).

[116] B. I. Schneider, T. N. Rescigno, and C. W. McCurdy, Phys. Rev. A **42**, 3132 (1990).

[117] S. Mahalakshmi and M. K. Mishra, Chem. Phys. Lett. **296**, 43 (1998).

[118] S. Kaur and K.L. Baluja, J. Phys. B **38**, 3917 (2005).

[119] M. Vinodkumar, H. Bhutadia, B. Antony, and N. Mason, Phys. Rev. A **84** (2011).

[120] G. A. Gallup, Phys. Rev. A **84**, 012701 (2011).

[121] C. R. Claydon, G. A. Segal, and H. S. Taylor, J. Chem. Phys. **52**, 3387 (1970).

[122] L. Sanche and G. J. Schulz, J. Chem. Phys. **58**, 479 (1973).

[123] M. J. W. Boness and G. J. Schulz, Phys. Rev. A **9**, 1969 (1974).

[124] M. Allan, Phys. Rev. Lett. **87**, 033201 (2001).

[125] K. Aflatooni, B. Hitt, G. A. Gallup, and P. D. Burrow, J. Chem. Phys. **115**, 6489 (2001).

[126] P. D. Burrow and L. Sanche, Phys. Rev. Lett. **28**, 333 (1972).

[127] S. Denifl, V. Vizcaino, T. D. Märk, E. Illenberger, and P. Scheier, Phys. Chem. Chem. Phys. **12**, 5219 (2010).

[128] Y. Yoshioka, H. F. Schaefer, and K. D. Jordan, J. Chem. Phys. **75**, 1040 (1981).

[129] T. N. Rescigno, D. A. Byrum, W. A. Isaacs, and C.W. McCurdy, Phys. Rev. A **60**, 2186 (1999).

[130] T. N. Rescigno, W. A. Isaacs, A. E. Orel, H.-D. Meyer, and C. W. McCurdy, Phys. Rev. A **65**, 032716 (2002).

[131] A. Moradmand, D. S. Slaughter, D. J. Haxton, T. N. Rescigno, C. W. McCurdy, T. Weber, S. Matsika, A. L. Landers, A. Belkacem, and M. Fogle, Phys. Rev. A **88**, 032703 (2013).

[132] L. A. Morgan, Phys. Rev. Lett. **80**, 1873 (1998).

[133] M. A. Morrison, N. F. Lane, and L. A. Collins, Phys. Rev. A **15**, 2186 (1977).

[134] R. R. Lucchese and V. McKoy, Phys. Rev. A **25**, 1963 (1982).

[135] C.-H. Lee, C. Winstead, and V. McKoy, J. Chem. Phys. **111**, 5056 (1999).

[136] F. A. Gianturco and T. Stoecklin, J. Phys. B **29**, 3933 (1996).

[137] K. D. Jordan and P. D. Burrow, Chem. Rev. **87**, 557 (1987).

[138] D. Mariano, A. Vera, and A. B. Pierini, Phys. Chem. Chem. Phys. **6**, 2899 (2004).

[139] E. Epifanovsky, I. Polyakov, B. L. Grigorenko, A. V. Nemukhin, and A. I. Krylov, J. Chem. Theory Comput. **5**, 1895 (2009).

[140] D. Zuev, K. Bravaya, M. Makarova, and A. I. Krylov, J. Chem. Phys. **135**, 194304 (2011).